

© 2011 Andrew Joseph Nelson

BENCH-SCALE EVALUATION OF AN ENERGY EFFICIENT
ACOUSTIC AEROSOL PURIFICATION DEVICE WITH
A NEWLY DESIGNED BIOAEROSOL TESTING AND EVALUATION CHAMBER

BY

ANDREW JOSEPH NELSON

THESIS

Submitted in partial fulfillment of the requirements
for the degree of Master of Science in Environmental Engineering in Civil Engineering
in the Graduate College of the
University of Illinois at Urbana-Champaign, 2011

Urbana, Illinois

Adviser:

Professor Mark J. Rood

ABSTRACT

The most common method to purify building air of particulate matter is fabric filtration that can cause a large pressure drop, resulting in high-energy use for adequate protection. Facilities requiring advanced protection against particulate matter typically utilize high efficiency particulate air (HEPA) filters capable of removing 99.97% of particles larger than 0.3 μm in diameter. These filters have high associated energy costs due to pressure drop and can become contaminated with potentially hazardous material during normal operation. Hence, it is important to test alternative low pressure drop (LPD) methods that treat indoor air streams to achieve high particle removal efficiencies while also achieving high operational stability.

A bench-scale test chamber has been designed, assembled, and validated for the evaluation of operational characteristics of novel LPD filtration technologies at flow rates up to 50 CFM (1.4 m^3/min) including removal efficiency, pressure drop, and power consumption. The chamber is based on ASHRAE Standard 52.2 and is carefully designed to meet all validation metrics put forth in the standard. Aerosol particle removal technologies can now be tested at the bench-scale over a range of operating conditions to assess the effects of flow rate and power on collection efficacy. Additionally, these technologies can be evaluated for viability of retrofit installation and maintenance. Based on results from bench-scale investigations, the LPD filtration technologies will be evaluated further in a relevant environment simulated at a pilot-scale test-bed facility, in cooperation with the Department of Defense Joint Program for Collective Protection.

In this research, a novel Acoustically Enhanced Impaction (AEI) air purification technology is evaluated as a potential alternative to HEPA filtration in building protection applications. AEI utilizes intense sound fields to induce aerosol drift and enhance probability of impaction on coarse filter media to collect the particulate matter within the device. The newly designed test chamber was implemented to characterize pressure drop, graded particle removal efficiency, and power requirements of the AEI. These results were compared to pressure drop and graded particle removal efficiency of conventional HEPA filters based on data available in the literature. A cost analysis was prepared to compare annualized operational cost of the current first-generation AEI device with commercially available HEPA filtration. Finally, projected

annualized operational cost was calculated and compared for the AEI device, HEPA filtration, and an Electro spray Enhanced Impaction (EEI) method of air purification.

The test chamber was also developed to evaluate an EEI system for energy efficient air purification. EEI utilizes electro spray ionization of particles followed by downstream collection on charged plates. This device will be tested in the near future once it can be interfaced with the test chamber.

To Kate and our canine kids.

ACKNOWLEDGEMENTS

There are many people who are deserving of my thanks in writing, and I surely cannot list them all here. Dr. Mark Rood and the University of Illinois Air Quality Engineering and Science Group members provided their thoughtful input during the work and helped me to frame my ideas. Mr. Benjamin Brem was invaluable for his knowledge and assistance in aerosol generation and measurement techniques. It was only with his help that I was able to so carefully calibrate my own instruments prior to measurement. Mr. Mark Ginsberg, Dr. Martin Page, Dr. Kathryn Guy, and the U.S. Army ERDC/CERL Chemical and Biological Infrastructure Protection Team helped me to develop and implement ideas and understand the importance of this work and how it will help the Army and the Nation. Dr. Ashok Kumar has taught me many lessons about both work and school life while acting as my mentor from day one. And last but not least I would be remiss if I did not thank my family and friends for their support, encouragement, and faith in me as I continue my education. This work was supported by the Defense Threat Reduction Agency Project# BA09PHM900, Bioprotection of Facilities.

TABLE OF CONTENTS

LIST OF FIGURES	viii
LIST OF TABLES	x
1. INTRODUCTION	1
1.1. Motivation.....	1
1.2. Bioaerosols.....	2
1.2.1. <i>Characteristics of Bioaerosols</i>	3
1.3. Indoor Air Purification Methods.....	3
1.3.1. <i>Fabric Filtration</i>	3
1.3.2. <i>Electrostatic Precipitation</i>	5
1.4. Current Protection Strategies	6
1.4.1. <i>Available Guidelines</i>	6
1.4.2. <i>Sensors</i>	7
1.4.3. <i>HVAC Augmentation</i>	7
1.5. New Air Purification Devices.....	8
1.5.1. <i>Acoustically Enhanced Impaction</i>	9
1.5.2. <i>Electrospray Enhanced Impaction</i>	11
1.6. Research Objectives.....	12
2. MATERIALS AND METHODS.....	14
2.1. Bioaerosol Testing and Evaluation Chamber Design	14
2.1.1. <i>ASHRAE Method 52.2</i>	14
2.1.2. <i>Bio-TEC Design</i>	14
2.2. Aerosol Generation	15
2.3. Aerosol Sampling.....	16
2.4. Flow, Pressure, and Power Measurements	19
2.5. Aerosol Measurement Equipment Validation.....	19
2.5.1. <i>LAS Sizing Accuracy</i>	19
2.5.2. <i>LAS Number Concentration Accuracy</i>	20
2.5.3. <i>Sample Train Flow</i>	20
2.6. Bio-TEC Characterization	21
2.6.1. <i>Background Aerosol Concentration</i>	21

2.6.2.	<i>Uniformity of Face Velocity and Aerosol Concentration</i>	21
2.7.	Particulate Removal Efficiency	22
2.7.1.	<i>AEI Particle Removal Efficiency</i>	23
2.8.	Calculation of Annualized Operational Cost	24
3.	RESULTS AND DISCUSSION	25
3.1.	Interpretation of ASHRAE Method 52.2	25
3.1.1.	<i>Terminal Settling Velocity of KCl</i>	25
3.1.2.	<i>Total Gas Residence Time</i>	28
3.1.3.	<i>Reynolds Number</i>	29
3.2.	Design and Assembly of Bio-TEC	29
3.2.1.	<i>Bio-TEC Segment Design</i>	29
3.2.2.	<i>Material Properties</i>	31
3.2.3.	<i>Flow Generation</i>	32
3.3.	Aerosol Generation	33
3.4.	Aerosol Sampling Equipment	36
3.4.1.	<i>Isokinetic Sampling Ports</i>	36
3.4.2.	<i>Dilution and Analysis with LAS</i>	37
3.5.	Equipment Calibration and Validation	38
3.5.1.	<i>LAS Sizing Accuracy</i>	38
3.5.2.	<i>LAS Number Concentration Accuracy</i>	39
3.5.3.	<i>Flow Rates in Sample Train</i>	40
3.5.4.	<i>Bio-TEC Background Concentration</i>	40
3.6.	Characterization of AEI Device	41
3.7.	Cost Analysis	44
4.	SUMMARY AND CONCLUSIONS	49
4.1.	Summary of Research Results	49
4.2.	Future Work	50
5.	REFERENCES	52
	APPENDIX A: SCHEMATICS OF BIO-TEC SECTIONS	55

LIST OF FIGURES

Figure 1.1: Illustration of mechanisms for removal of particles by a single collector body. In the figure the collector body is negatively charged to illustrate electrostatic deposition of a positively charged particle	4
Figure 1.2: Array of nine acoustic flow-through channels arranged into an array (image adapted with permission from the original author).....	10
Figure 1.3: Electrospray ionization of particles in an air stream	11
Figure 1.4: Complete operational concept of EEI system	12
Figure 2.1: Flow diagram of Bio-TEC segments.....	15
Figure 2.2: Nipple (in red box) connecting drying column to Bio-TEC	16
Figure 2.3: Schematic of aerosol sampling train including sample extraction from Bio-TEC, dilution, wye, laser aerosol spectrometer (LAS), and pump	18
Figure 2.4: Sampling points for calibration of sample train	21
Figure 2.5: Nine-section traverse for measuring face velocity and aerosol concentration	22
Figure 3.1: Theoretical terminal settling velocity as calculated with Eq. 10.....	26
Figure 3.2: Comparison of particle removal efficiency under laminar and turbulent flow conditions.....	27
Figure 3.3: Photograph of complete Bio-TEC with main components highlighted. The flow generation and pre-filtration sections are located out of the image on the left side	30
Figure 3.4: Three sections of the Bio-TEC coupled with clamps. The flanges are gasketed with a closed cell foam material	31
Figure 3.5: Vertical orientation of the blower and HEPA pre-filtration stage prior to Bio-TEC connection via conductive tubing.....	33
Figure 3.6: Data confirming the presence of a polydisperse aerosol from 0.5 - 1.5 μm in diameter.....	34
Figure 3.7: Aerosol inlet and mixing – computer aided design (CAD) drawing of chamber sections at the aerosol inlet. Test aerosol enters through the nipple at the top left. Flow is from left to right.....	35
Figure 3.8: Outlet of aerosol diluter modified for in-line use.....	37

Figure 3.9: Image of diluter, wye, laser aerosol spectrometer (LAS), and pump flow direction for sampling equipment	38
Figure 3.10: LAS Calibration – measured particle diameter from the LAS compared with NIST-traceable PSL particle standards	39
Figure 3.11: Prevalence of background aerosol in the Bio-TEC presented as total particle counts in each size bin during a 5 min sample while withdrawing sample at 3,000 cm ³ /min and sampling at 180 cm ³ /min	41
Figure 3.12: AEI removal efficiency vs. power for 0.5-1.5 μm diameter particles. Standard deviations, noted by vertical lines are too small to see for all test conditions except 540 W. Particle removal efficiency values achieved when the device is not powered on are not included in this figure.....	43

LIST OF TABLES

Table 1.1: CDC list of bioterrorism agents and diseases by category	2
Table 3.1: Residence times calculated at lowest flow for ASHRAE Method and Bio-TEC. Section locations correspond to the diagram presented in Figure 3.3	28
Table 3.2: Sizes of sample ports for varying Bio-TEC flow rates.....	36
Table 3.3: Measured flow rates at key points in sample train at actual conditions	40
Table 3.4: Annualized cost of AEI device compared with clean and dirty HEPA filtration.....	45
Table 3.5: Estimated annualized operational costs for second generation AEI air purification technology and EEI device based on vendors anticipated energy requirements. Costs are estimated based on electricity price of \$0.15 per kWh	47

1. INTRODUCTION

1.1. Motivation

Attack by hostile nations or terrorist groups using biological warfare agents (BWA) has been defined by the President of the United States, Department of Homeland Security, and the Department of Defense as a legitimate threat to the Nation.^{1,2} Events such as the aerosolized release of *Bacillus anthracis* (anthrax) in Tokyo, Japan in 1993, the World Trade Center attack in 2001, and anthrax-laden letters sent to members of Congress demonstrate the unpredictable nature of threats in the modern world.³ The uncertainty of an attack coupled with the relative ease of weaponization and dissemination of BWAs illustrates the need for effective protection against BWA threats.⁴

Protection of high-risk buildings from biological attack is important for national security. Many facilities both in the United States and abroad may be targets for attack. Programs such as the Pentagon Force Protection Agency's (PFPA) "Pentagon Shield" and the Defense Advanced Research Program's (DARPA) Immune Building project have utilized a sophisticated network of sensors coupled to air handling equipment and decontamination strategies to provide a complete protection system known as collective protection.^{5,6,7} While these systems provide increased protection from attack by a chemical or biological warfare agent, they are not practical for use in wide-ranging applications.

Although major buildings such as the White House, Pentagon, and United States Capital Building have some degree of protection from BWAs, many smaller or mobile facilities do not have increased protection. Currently available systems are cost intensive and require significant operational and maintenance investments to effectively operate a 100% duty cycle. It is estimated that the addition of a complete system for protection against BWAs will increase capital cost of a building by up to 30%.^{4,2} Additionally, many current protection strategies fail to address the infiltration of contaminants due to occupant ingress. A person moving into a building from a contaminated outdoor environment will carry a wake of outdoor air inside. This wake contains outdoor contaminants and is an important factor in designing building protection strategies.⁶ In order to provide enhanced biological protection to more facilities, an approach

with lower capital and operational costs needs to be realized to be more efficient with respect to cost and energy consumption.

1.2. Bioaerosols

There are over 1,400 known infectious organisms, 700 of which are potentially pathogenic.² The United States Centers for Disease Control and Prevention (CDC) has categorized infectious organisms according to their potential for use as BWAs and ability to cause widespread public health disruptions. Potential BWA threats are divided into three groups, Category A, B, and C, based on the potential of the agent as a threat for widespread dissemination with high morbidity and mortality rates. Threats of highest priority (Category A) agents are those which are a potential threat to national security, including anthrax, botulism, and plague.⁸

Table 1.1: CDC list of bioterrorism agents and diseases by category⁸

<p>Category A: “Highest priority agents include organisms that pose a risk to national security”</p> <ul style="list-style-type: none"> • easily disseminated • high mortality rates • cause public panic/disruption • require special action for preparedness 	<p>Anthrax Botulism Plague Smallpox Tularemia Viral hemorrhagic fevers</p>
<p>Category B: “Second highest priority agents”</p> <ul style="list-style-type: none"> • moderately easy to disseminate • moderate morbidity, low mortality rates • require specific enhancements for diagnosis 	<p>Brucellosis Epsilon toxin Food safety threats (<i>E. coli</i>, <i>Salmonella</i>) <i>Glanders</i> <i>Melioidosis</i> <i>Psittacosis</i> <i>Q fever</i> <i>Ricin toxin</i> <i>Staphylococcal enterotoxin B</i> Typhus Fever Viral encephalitis Water safety threats (cholera, crypto, etc.)</p>
<p>Category C: Third highest priority includes emerging pathogens with potential future use in wide dissemination for high morbidity and mortality rates and major public health impact. This includes emerging infectious diseases such as hantavirus and Nipah virus.</p>	

1.2.1. *Characteristics of Bioaerosols*

Aerosolization of a typical bacterial spore from an aqueous solution yields rod-shaped particles ranging in length from 1 to 8 μm .⁹ Particles of this size are easily inhaled and entrained in the human respiratory system. Inhalation of as few as 2,000 anthrax spores can cause illness in humans.¹⁰ Because the onset of illness is related to total number of spores inhaled, reducing or eliminating exposure is key to limiting spread of infection. Additionally, initial symptoms of BWA exposure are similar to the flu and only become more specific to the agent as post-exposure time passes when treatment options become limited.²

1.3. Indoor Air Purification Methods

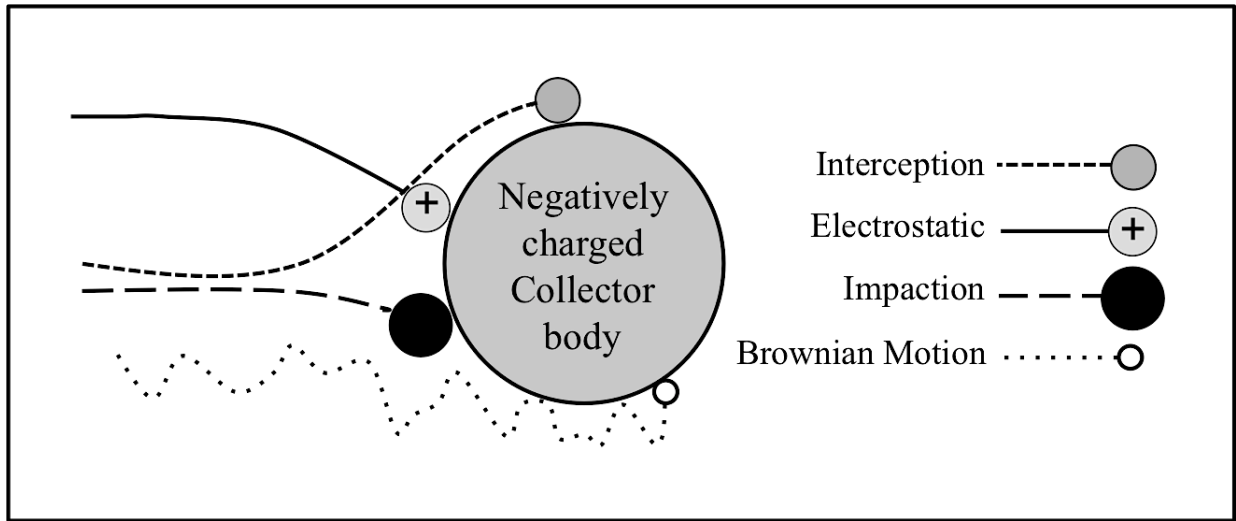
Traditional methods of building protection from external pollutants are limited to fabric filters and electrostatic precipitators (ESPs).¹¹ These systems are commonly utilized in indoor environments and each has unique capabilities and drawbacks.

1.3.1. *Fabric Filtration*

Fabric filters are commonly used to separate particulate matter from an air stream in a building environment. They are commonly used to purify air in homes and commercial and industrial environments.¹³ Particles are collected on fabric filter media by impaction, interception, or Brownian motion.¹² Depending on particle diameter and charging, any one of these phenomena may dominate collection.

Impaction occurs when a particle comes into direct contact with the collection body. This occurs most readily for particles where the inertial force prevents them from following the fluid streamlines around a collector body. Interception occurs when particles are able to follow the fluid streamline around the collector but ultimately contact the collector because of their size. Diffusion is most dominant for small particles and is characterized by the random motion of particles in the gas stream that causes them to contact the collector body. Electrostatic forces occur when a charged particle is drawn to an oppositely charged collector body and act to enhance collection by impaction, interception, and Brownian motion.

Figure 1.1: Illustration of mechanisms for removal of particles by a single collector body. In the figure the collector body is negatively charged to illustrate electrostatic deposition of a positively charged particle



The use of high efficiency particulate air (HEPA) filters has been demonstrated to be effective at removing 99.97% of particles larger than $0.3\mu\text{m}$ in diameter, it is well documented that the pressure drop due to filter packing and subsequent filter cake buildup during operation leads to an undesirable increase in building energy requirements.^{11,13} For applications where the need for protection is primary and cost is secondary, HEPA filters may be a good fit. However, in most applications they are prohibitively expensive to operate and are not economically feasible for wide-scale applications. This project seeks to reduce operation and maintenance costs by at least an order of magnitude over HEPA filtration for equivalent or improved protection.

Fabric filter media are generally effective at capturing nanoscale particles by diffusion and particles larger than $1\mu\text{m}$ diameter by interception and impaction.¹³ There is a minimum in filtration efficiency that normally occurs for particles of about $0.5 - 1\mu\text{m}$ diameter^{14,15}. This minimum of collection efficiency overlaps with the size range of many BWAs of interest. Therefore, fabric filters are often limited in their ability to adequately protect from BWAs because of significant reduction in collection efficiency in that size range. For example, collection efficiency of $0.5\mu\text{m}$ diameter particles by a polycarbonate filter with $1\mu\text{m}$ pore diameter has been reported as 55% of the measured overall mass collection efficiency for $2\mu\text{m}$ diameter particles.

1.3.2. *Electrostatic Precipitation*

ESPs have a unique capability to remove particles at or near HEPA efficiencies without the associated pressure drop due to an open flow through design.¹³ ESPs utilize electrostatic forces to attract particles to a collection surface and separate the particles from the gas stream. There are three main steps to ESP air purification. Incoming particles are ionized to impart a charge for collection. Ionization is accomplished by establishing a corona discharge to initiate an electron avalanche that ionizes electronegative gases in the gas stream. The negatively charged gas ions then attach onto particles. Charged particles are then passed through a collection region where they are electrostatically deposited on charged plates. Finally, the collected particles must be removed from the collection plates to allow for continuous purification.¹²

ESPs are typically designed in one of two configurations. A single-stage ESP ionizes particle and collects them in the same region. A two-stage system ionizes and collects particles in two distinctly separate regions. In both applications, particle ionization is typically achieved by using a corona discharge in the charging region.¹⁶ For treatment of indoor air in buildings, two-stage ESPs are the most common design.^{17,20} Therefore, discussion in this paper will be limited to operational characteristics of two-stage precipitators.

While corona discharge is an effective mechanism for imparting charge to airborne contaminants, it is known to produce tens of parts per billion of ozone under normal operating conditions.^{18,19} Ozone is a strong oxidizing agent and is highly reactive in the environment.¹⁹ A typical indoor environment contains only trace levels of ozone.²² Operation of two-stage ESPs in indoor environments has been shown to generate at least 20 ppb_v of ozone to the indoor environment.²⁶ The process of ozone generation starts when an electron of approximately 6eV from the corona discharge causes the dissociation of molecular oxygen (Eq. 1). Ozone is formed when the atomic oxygen combines with molecular oxygen (Eq. 2).²⁰



The Occupational Safety and Hazards Administration limits indoor ozone levels to 100 ppb_v during an 8-hour work day.²⁰ Additionally, Title 21 of the Code of Federal Regulations set the maximum acceptable level of ozone added to an indoor environment by an air cleaning device to 50 ppb_v.²¹ Elevated ozone in buildings has been shown to lead to an increase in the concentration of airborne particles²² as well as the creation of potentially harmful secondary organic aerosols from reactions with other indoor contaminants.^{16,19,20} Ozone has deleterious effects on the heart, nervous system, and vision and is known to be an irritant to mucous membranes. Therefore, while ESPs are effective at capturing particles in the size range common to BWAs, the production of ozone during operation makes them problematic for indoor air purification applications.

1.4. Current Protection Strategies

Many systems currently used for building protection from BWAs utilize a suite of technologies including, but not limited to, a sensor package, augmented heating, ventilation, and air conditioning (HVAC) system, and active decontamination equipment. For buildings not equipped with technologies designed for biological protection, there are often simple measures that can be taken to mitigate the threat associated with BWAs as described in section 1.4.3.

1.4.1. Available Guidelines

The CDC and the National Institute for Occupational Safety and Health (NIOSH) have published a handbook outlining strategies for building protection from chemical, biological, and radiological attack.²³ The recommendations in this document provide a minimal level of added protection. Most protection methods are focused on modified approaches to physical security and building design to prevent direct access to building HVAC equipment. Physical security guidelines such as these are designed to limit access to key BWA entry points by terrorists. These guidelines are primarily directed to facility managers who seek an increased level of protection but have limited funding to implement new technology.

1.4.2. *Sensors*

Biological agent detectors used in a sensing network are divided into two main categories: point detectors and standoff detectors. Point detectors require the extraction of a sample for analysis, while standoff detectors are capable of sensing threats remotely. Point detectors are useful for analysis of a known potential threat (e.g., local monitoring for contamination by a chemical plant) but are ineffective for direct and rapid detection of an unknown threat because of their limited ability to detect an agent over a wide spatial area such as a city or region.^{2,5} Spatial limitations are primarily driven by cost of individual devices. The highest attainable resolution is a direct function of the number of detectors within the area of interest. These sensors are often referred to as “detect to treat” because they are used to determine specific agents *after* an attack is confirmed.

Standoff detectors (“detect to warn”) identify a threat *before* it has reached the area of interest, allowing for enhanced protection and responsive action²⁴. These sensors are capable of providing vital information during the early development of a threat and allow for use of low-risk protection methods based on preliminary detection information. Standoff detectors measure unique optical properties of biological aerosols to distinguish them from other atmospheric particles and provide real time information about developing threats.

1.4.3. *HVAC Augmentation*

The CDC/NIOSH handbook provides recommendations for upgrades to HVAC systems that can increase biosecurity of a building. This includes active HVAC control systems, upgrading filtration capability, and reducing leakage of HVAC dampers and building envelope by upgrading seals at doors and windows or utilizing “air curtains” at entryways to reduce air exchange between the building and external environment.

Active HVAC control systems may be effective at reducing the spread of BWAs through a building if they are used appropriately. In cases where contamination is limited to a small portion of the building, it may be useful to provide negative pressure in that area to reduce contaminant transport.²³ While this can be a useful technique to reduce the overall footprint of

an attack, many buildings are not equipped with active controls or adequate zoning of HVAC ducting.

Active controls require that any decision to modify localized building pressure to mitigate the spread of contamination be made quickly to be effective.²⁵ Unless the dissemination of a BWA is witnessed and reported, it is likely that active HVAC controls will not be effective for protection in the absence of an extensive sensor network. Shutdown of HVAC equipment during a BWA attack, known as the “shelter-in-place” approach can reduce the transport of BWAs through building ductwork. However, it has been shown that even a well-sealed building is prone to penetration by spore-sized biological material in the absence of building overpressure.²⁶

While the use of upgraded filtration equipment capable of collecting a higher percentage of sub- μm diameter particles may be effective for increased protection, it would likely require extensive upgrades to the air handling unit (AHU) and associated HVAC equipment. When using traditional filtration methods, an increase in filtration efficiency is generally linked to an increase in pressure drop across the filter due to the formation of a filter cake caused by the captured particulate matter. Replacing moderate efficiency filters with a media such as HEPA filters will reduce the air recirculation rates in the building and increase stress on the mechanical components of the HVAC system. Due to increased pressure drop caused by HEPA filters, in duct flow rate will be reduced if the blower is not appropriately sized. Therefore, an upgraded filtration system with an increased static pressure would likely also require an upgraded AHU fan to compensate for added pressure.²⁷

1.5. New Air Purification Devices

This research is focused on the description of two novel Low-Pressure Drop (LPD) air purification devices and the careful evaluation of one of those devices to determine if it can achieve particle collection efficiencies comparable to HEPA filtration at reduced energy consumption. A second LPD device will be tested upon receipt of the equipment needed to test the device. These two technologies are acoustically-enhanced and electrospray-enhanced impaction (AEI and EEI, respectively).

AEI enhances particle movement and aerosol agglomeration in a flow-through cell by application of a sound field transverse to the direction of airflow. The intensified particle motion increases the probability of particle impaction on coarse filter media within the device.²⁸

The EEI method is similar to an ESP, but utilizes an electrospray wick system instead of corona discharge to ionize particles. This design is capable of imparting charge without releasing ozone into the environment because of the reduced electric field strength required to generate the ions that charge the particulate matter.¹¹ Because of this difference in charging mechanism, EEI is capable of collection efficiencies similar to traditional ESPs with the added benefit of theoretically ozone-free operation.¹⁶

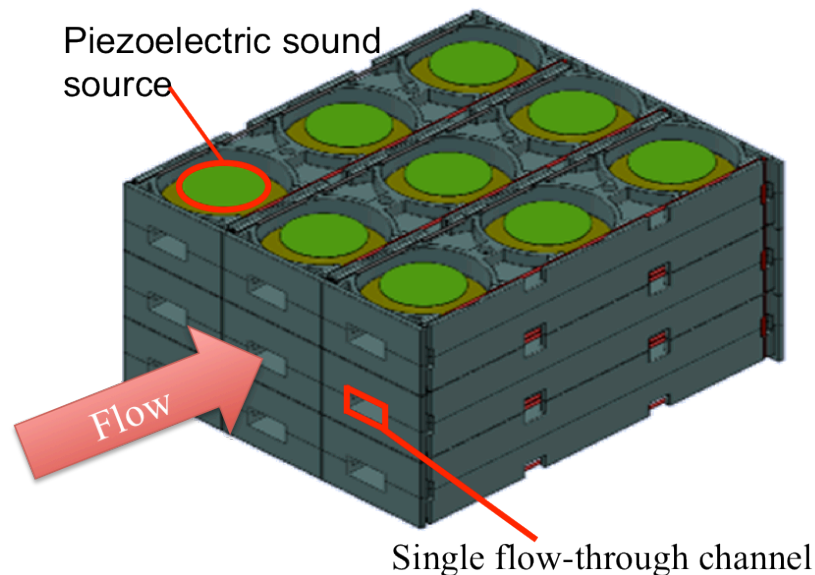
1.5.1. *Acoustically Enhanced Impaction*

It is well documented that acoustic radiation pressure can induce movement of an aerosol in a fluid stream.²⁹ Acoustic forces have been used to concentrate particles prior to optical sizing³⁰, sort particles for flow cytometry³¹, or to agglomerate aerosolized particles for enhanced deposition from air. Acoustic field-flow fractionation divides a particle laden flow stream into different parts depending on aerosol particle properties, particularly size and density. During fractionation, flow is directed down a channel with a sound source on one side. As the particles enter the sound field, they move transverse to the flow direction. Depending on the characteristics of the particles, they migrate to either a nodal or anti-nodal position within the sound field. Biological organisms such as bacteria, spores, and viruses that are common BWA threats have been shown to migrate to acoustic sound pressure nodes.

Recently, sound fields have been utilized to design a device capable of removing sub- μm diameter particles from a continuous flow air stream.²⁸ The AEI device, developed by Applied Research Associates (Littleton, CO), utilizes an inexpensive low pressure drop coarse filter media placed inside of a flow-through resonator cavity. The flow-through channel has sound sources oriented transversely to the direction of flow. The application of the sound field to the flow through cell causes the particles to experience a more tortuous pathway through the filter media. This increased movement enhances the probability that a particle will impact the coarse media.

Sound pressure is produced with a commercially available piezoelectric transducer sound source. The sound source is housed in custom-designed injection molded plastic housing. Each flow through cell contains six sound sources. There are three sources mounted on opposing sides of the flow through channel for a total of six piezoelectric elements per flow channel (Figure 1.2). The front cross sectional area of the flow through channel is 0.75" x 0.375" (1.9 cm x 0.95 cm). The piezoelectric elements are driven at 3.2 kHz by a commercially available audio amplifier.

Figure 1.2: Array of nine acoustic flow-through channels arranged into an array (image adapted with permission from the original author)³²



The design of the system is based on smaller “building blocks” that can be stacked to operate cooperatively. This allows for a simple scale-up design where many sections are stacked together for increased flow of contaminated air.

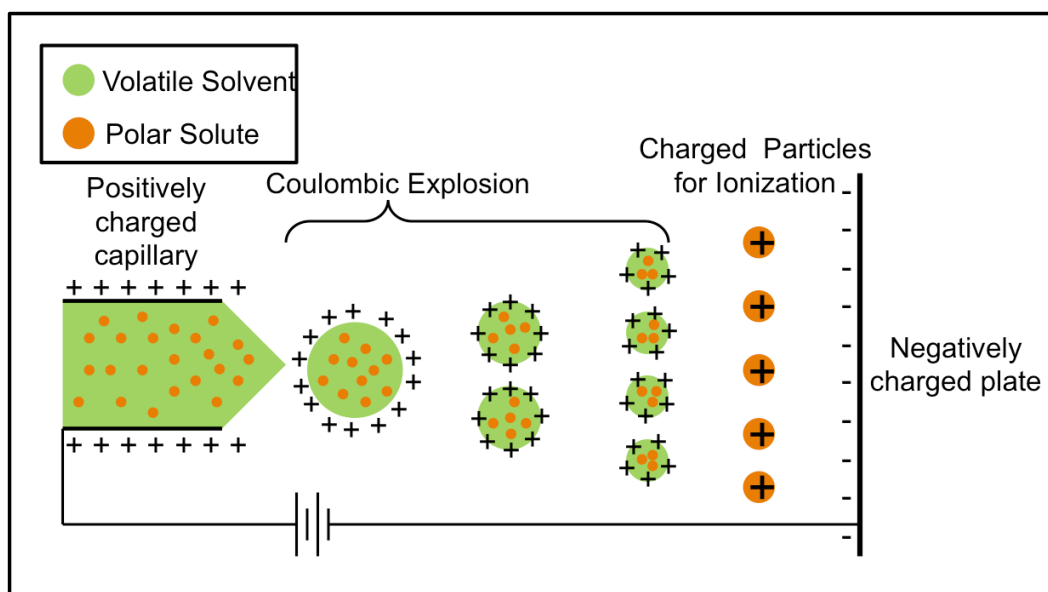
Because the AEI device is intended for use in building HVAC applications, it is important that operation of the device does not add significant noise pollution to the building. The device is capable of producing 160 dB sound pressure inside the flow chamber. This sound pressure level is dangerous even under short exposures. Therefore, a sound dampening system was designed

and integrated into the system by the manufacturer prior to delivery. The added sound dampening material resulted in an ambient sound pressure of 68 dB during device operation.

1.5.2. *Electrospray Enhanced Impaction*

Electrospray Ionization (EI) is typically used in the field of analytical chemistry for sample preparation during mass spectrometry.³³ EI utilizes a solute dissolved in a volatile solvent that is drawn through a charged capillary channel and sprayed into the atmosphere. The capillary has a strong positive voltage that in turn charges the liquid solvent. The liquid is drawn from the capillary by negatively charged plate. After it is sprayed from the capillary tip, the charged liquid forms μm diameter-sized, positively charged droplets. Next, the volatile solvent rapidly evaporates and the droplet undergoes a series of Coulombic explosions that occur when the energy from droplet's electrostatic charge exceeds its energy from liquid surface tension.³⁴ The Coulombic explosions are repeated and a nanoscale charged droplet is formed. These nanoscale droplets attach to polar or polarizable constituents in the air stream and ionize them for collection.^{11,35}

Figure 1.3: Electrospray ionization of particles in an air stream

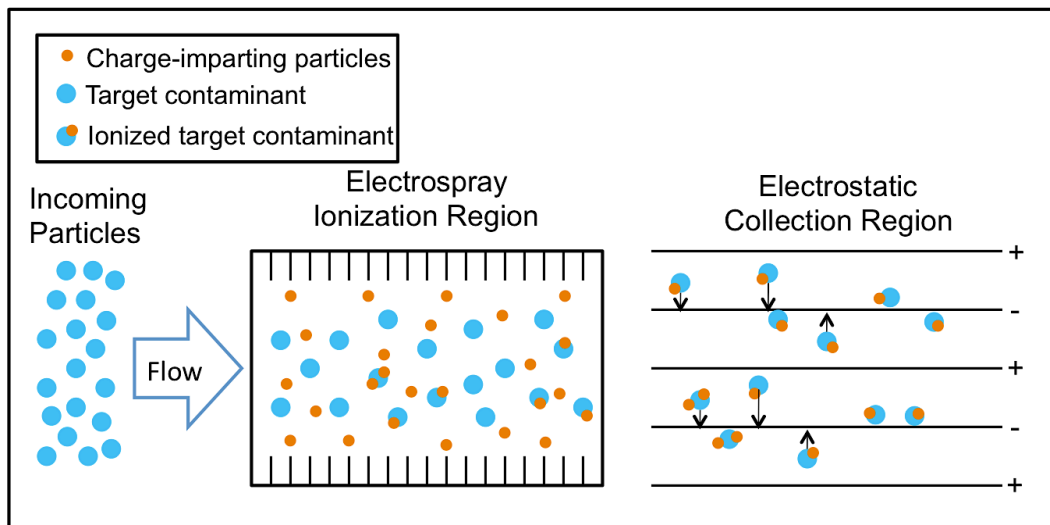


EI has been used as an alternative ionization method in a two-stage ESP.¹¹ Because the charged droplets only attach to polar or polarizable species, the system does not ionize nitrogen or

oxygen in the air and operates without the formation of additional ozone.¹¹ During operation of the device, no measurable increase in ozone is detected.^{16,36}

The EEI method of air purification is designed similarly to a two-stage ESP (Figure 1.4). Incoming particles first pass through a charging region where they are ionized with an EI system. As the ionized particles travel downstream, they enter a collection region composed of parallel stainless steel plates with an established electric field.

Figure 1.4: Complete operational concept of EEI system



1.6. Research Objectives

This research develops and characterizes a bench-scale chamber for testing and evaluation of newly developed air purification technologies for potential continuous 24 hr/day and 7 day/week building protection applications. Two systems are proposed for air purification that add minimal pressure drop and are capable of long term operation with few consumables and nominal maintenance burden. The bench-scale chamber was designed, fabricated, and calibrated to assess candidate technologies at flow rates up to 50 CFM (1.4 m³/min). The specially designed chamber allows for evaluation of technologies at their current bench-scale, and the data generated in this system will guide future pilot-scale evaluations at a representative building under various attack scenarios. The chamber was used to characterize pressure drop, graded particle removal efficiency, and power requirements of a first generation AEI device. These

results were compared with pressure drop and graded particle removal efficiency for conventional HEPA filtration. A cost analysis was also prepared to compare annualized operational cost of the AEI device with HEPA filtration based on measured pressure drop and power requirements.

2. MATERIALS AND METHODS

2.1. Bioaerosol Testing and Evaluation Chamber Design

2.1.1. *ASHRAE Method 52.2*

Use of ASHRAE Method 52.2 is the accepted approach for in-duct testing of air purification equipment to yield a standardized comparison metric.³⁷ It provides a technique for laboratory testing of removal efficiency of polydisperse aerosol particles 0.30 to 10 μm in diameter at airflow rates between 472 cfm and 3,000 cfm (13.4 to 141.6 m^3/min). Both air-purification devices evaluated in this study exist only at the bench scale, and are not capable of treating air in excess of 50 cfm (1.4 m^3/min). Therefore, an experimental test chamber was required that could provide a standardized comparison at flow rates of 50 cfm (1.4 m^3/min). The ASHRAE Method 52.2 was used as a template to design and fabricate the Bioaerosol Testing and Evaluation Chamber (Bio-TEC). The Bio-TEC system is suitable for testing the devices of interest at their lower gas flow rate capabilities.

2.1.2. *Bio-TEC Design*

The Bio-TEC was designed after a thorough evaluation of the ASHRAE standard to reduce its scale. Key metrics of the ASHRAE test standard are aerosol mixing, flow stabilization and control, gas velocity measurement, and particulate matter concentration measurement. Other important characteristics included material selection, test aerosol, and measurement equipment. All chamber components including straightening, turn, and reduction segments were custom designed to replicate the ASHRAE standard at reduced scale.

The chamber was custom fabricated out of 16-gauge type 304 brushed stainless steel by a machine shop. To reduce aerosol loss during testing, the Bio-TEC was fabricated from electrically conductive material. After assembly of the Bio-TEC, the system was verified to have complete electrical continuity across all sections. This was confirmed by operating a handheld Scopemeter (192C Scopemeter Color, Fluke Corporation, Everett, WA) in “continuity check” mode to ensure electrical continuity across all adjacent sections.

The chamber was comprised of seven major sections: flow generation, pre-filtration, aerosol inlet, upstream mixing, air purification device, downstream mixing, and post-filtration (Figure 2.1).

The pre-filtration step was utilized to provide clean air for testing and the post-filtration section purified any residual test aerosol from the Bio-TEC airstream prior to releasing into the indoor environment. Upstream and downstream mixing sections were designed to provide turbulent mixing at all flow rates based on the calculated Reynolds number (Re) from Eq. 3.

$$Re = \frac{\rho_f V_C D_H}{\mu} \quad \text{Eq. 3}$$

where:

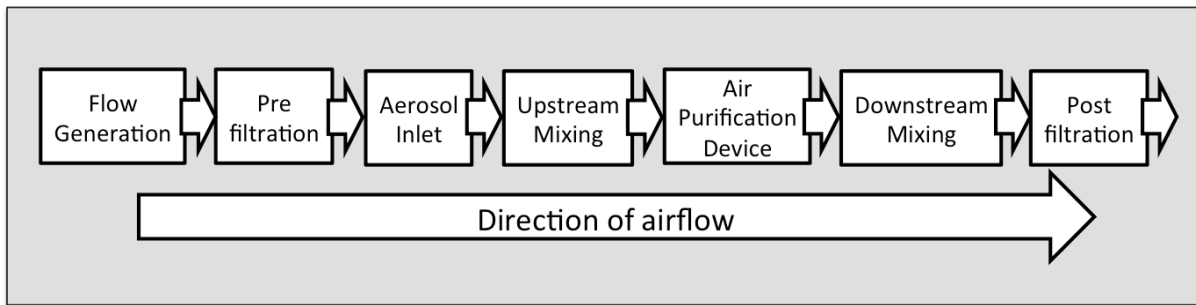
ρ_f = fluid density (kg/m³)

V_C = face velocity at the center of the chamber (m/s)

D_H = hydraulic diameter of chamber (m)

μ = dynamic viscosity of fluid (kg/m-s)

Figure 2.1: Flow diagram of Bio-TEC segments



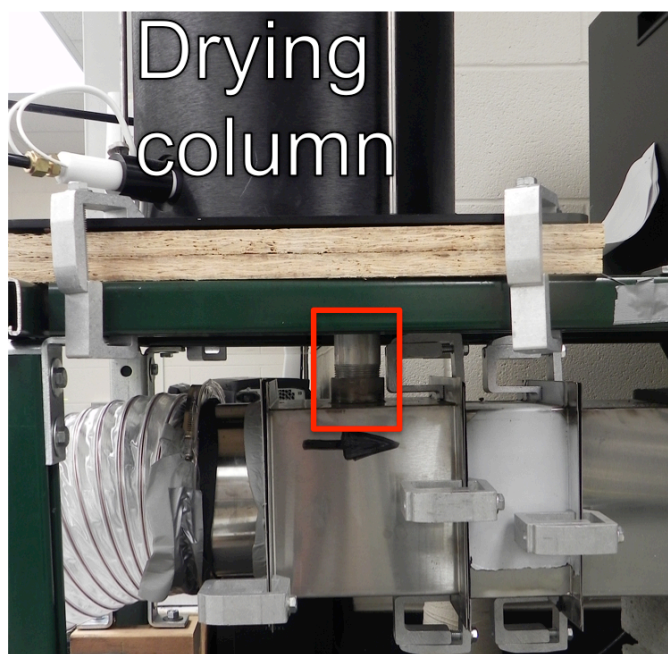
2.2. Aerosol Generation

Testing aerosols for evaluation of air purification equipment were generated based on the ASHRAE 52.2 standard. All test aerosols were generated with a TSI 8108 Large-Particle Aerosol Generator (TSI Inc., Shoreview, MN). An aqueous solution containing KCl (SigmaUltra $\geq 99.0\%$, Sigma-Aldrich, St. Louis, MO) solute in reagent grade deionized water (Acros Organics, Geel, Belgium) was utilized as a precursor for aerosol generation. KCl solution was drawn by a peristaltic pump and aerosolized at the top of a drying column. The atomized droplets fell counter current to a HEPA-filtered, charge neutralized, and heated air stream. The flow rate of the airstream was set so that it would slow, but not prevent,

gravitational settling of particles. During settling, the solvent evaporated from the aerosolized droplets. The solute then crystallized and dry KCl particles were formed.

The drying column was mounted on top of the Bio-TEC where aerosol settling occurred transversely to the direction of airflow in the test chamber. After crystallization of the aerosol, particles settled to the base of the drying column. An orifice at the base of the column was connected to an orifice on the top of the Bio-TEC system via a nipple. The aerosol was introduced via gravitational settling through the orifice and into the top of the Bio-TEC.

Figure 2.2: Nipple (in red box) connecting drying column to Bio-TEC



2.3. Aerosol Sampling

Continuously-streamed aerosol samples were extracted upstream and downstream of the air purification device. To minimize sample loss during extraction, all samples ports were designed to operate isokinetically with air flowing through the Bio-TEC. Therefore, a series of sample ports were designed and fabricated for use under varying flow rates. Sample ports were fabricated from type 304 stainless steel tubing.

Number concentration of samples was measured by a TSI 3340 Laser Aerosol Spectrometer (LAS). This equipment is capable of accurately measuring size and concentration of particles as small as 90 nm in diameter. It was operated via a LabView interface designed by TSI. The interface allowed for use controls of measurement size range from 90 nm to 10 μm in diameter. Upper and lower diameter limits of measurements are user-selectable. The device was capable of measuring up to 100 discrete particle size ranges. The LAS contained an internal pump capable of drawing aerosol flow up to 100 cc/min.

A dilution process was utilized for sampling. Samples extracted upstream of the air purification device were first diluted at a ratio of 100:1 using a TSI 3302A Aerosol Diluter. This was done because the air purification device under testing was expected to achieve greater than 99% collection efficiency of particles. This equipment used a capillary channel to split the incoming flow. Instead of adding makeup dilution air, the sample was diverted into two paths, one for sample air and one for dilution air. The dilution air was filtered twice by HEPA filters and then recombined with the sample stream. The equipment was designed for direct connection to a TSI Aerodynamic Particle Sizer (APS). Because an APS was not used in the sample train for the Bio-TEC, for this application the outlet was modified to allow connection to the optical particle sizing equipment.

To limit necessary equipment, upstream and downstream samples were both analyzed using the same LAS (Figure 2.3). A custom wye was designed to select which sample port was analyzed. The sample extracted upstream of the purification device was diluted prior to passing through the wye. Downstream samples were extracted and immediately passed through the wye. The wye was controlled manually by a straight ball valve (Ham-Let H6800 Series, Sugar Land, TX) installed immediately upstream for upstream of downstream sample selection. To ensure that the lines were clear of any residual upstream or downstream sample after switching, a waiting period was used each time the sample location was changed. The wait time was calculated with Eq. 4 and a safety factor of 20% was added to the calculated time.

$$t_w = \frac{CSA_S \times L_S}{Q_S} \quad \text{Eq. 4}$$

where:

t_w = waiting time (min)

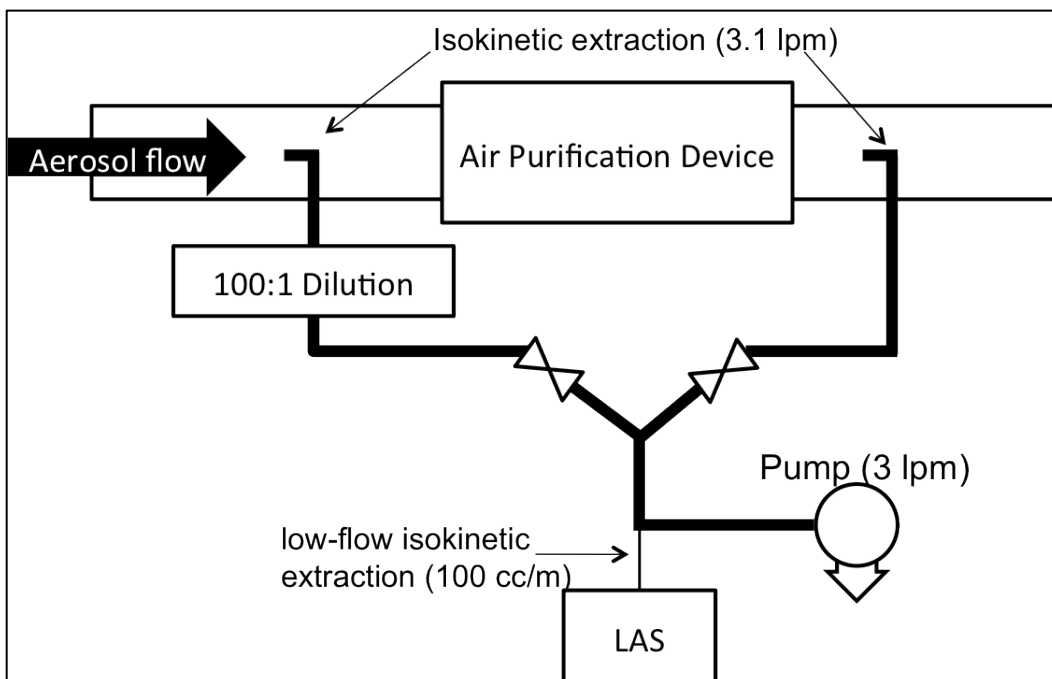
CSA_S = internal cross section area of sample tube (ft² or m²)

L_S = length of sample tube downstream of wye (ft or m)

Q_S = aerosol flow in sample tube (cfm or lpm)

Samples were extracted from the Bio-TEC with a Gast 0523 Vacuum Pump. Flow rate was controlled by a critical orifice provided with the TSI instrumentation located downstream of all measurement equipment. While the LAS was capable of inducing sample flow, the low internal flow capability of only 100 cc/min would likely cause significant loss of sample due to gravitational settling. Therefore, the vacuum pump was used to extract samples from the Bio-TEC and transport them to the LAS. Immediately upstream of the LAS, a low-flow sample was isokinetically extracted from the high flow sample line and fed to the measurement equipment.

Figure 2.3: Schematic of aerosol sampling train including sample extraction from Bio-TEC, dilution, wye, laser aerosol spectrometer (LAS), and pump



All sampling lines were made of conductive silicone tubing (Simolex Rubber Co., Plymouth, MI) to minimize aerosol loss by electrostatic deposition during transport.

2.4. Flow, Pressure, and Power Measurements

Airflow in the Bio-TEC was inferred from measurements of face velocity distribution over the chamber cross-section, using a TSI 9555 VelociCalc hot-wire anemometer.

$$Q_C = V_C \times CSA_C \quad \text{Eq. 5}$$

where:

Q_C = actual flow inside chamber (cfm or m³/min)

V_C = face velocity at the center of the chamber (ft/min or m/min)

CSA_C = cross sectional area of chamber (ft² or m²)

Pressure drop across the air purification device was monitored with a Dwyer D-1000 digital differential pressure gauge (Dwyer Instruments, Inc., Michigan City, IN). Total electrical power consumption for device operation was monitored “at the wall” with an AmWatt Load Tester (Reliance Controls, Racine, WI).

2.5. Aerosol Measurement Equipment Validation

Prior to installing and testing air purification devices in the Bio-TEC, equipment was validated for accuracy in measurements as a quality control measure.

2.5.1. LAS Sizing Accuracy

The LAS was tested independent of the Bio-TEC for accuracy in measuring particle sizes relevant to the test aerosol as well as total particulate concentration. Monodisperse polystyrene latex (PSL) spheres were aerosolized with a TSI 3076 Collison-type atomizer, dried, and charge neutralized. To determine accuracy in sizing, National Institute of Science and Technology (NIST) traceable PSL spheres (Polysciences, Inc., Warrington, PA.) were used. Concentrated PSL spheres were diluted in purified water (Barnstead Nanopure) and aerosolized. To reduce background noise, a TSI 3071 electrostatic classifier was used

upstream of the LAS to remove particles that were not in the range of the aerosolized spheres. As an additional validation step, the LAS was operated in parallel with a scanning mobility particle sizer (TSI 3936 with TSI 3071 Selector DMA and TSI 3010 Condensation Particle Counter with scanning chip) to ensure the calibration spheres were accurate in size and sufficiently monodisperse.

2.5.2. LAS Number Concentration Accuracy

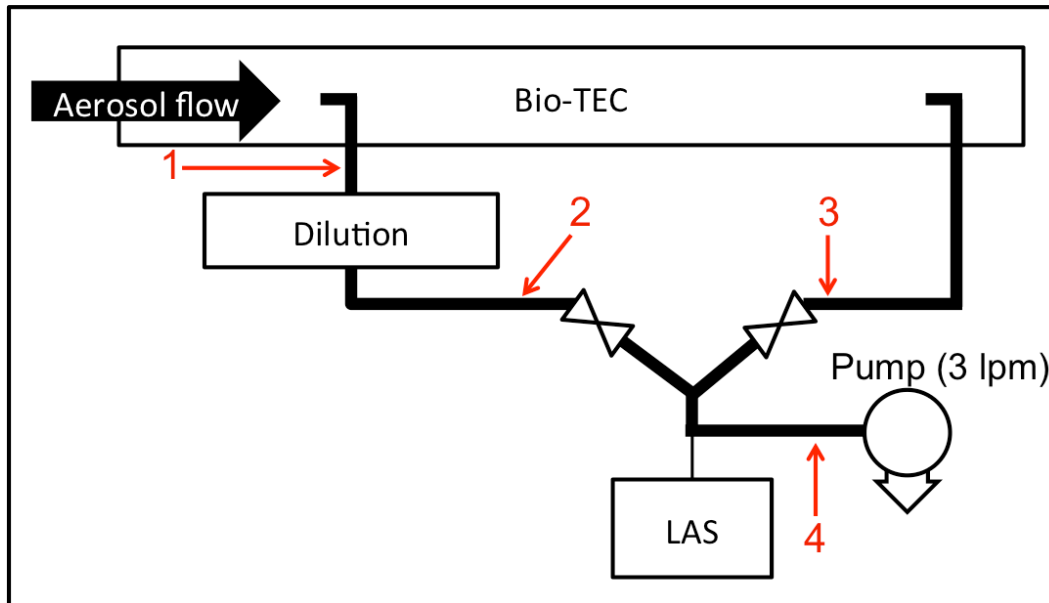
Using the same setup as described in section 3.2.1, a polydisperse aerosol was created to determine the accuracy of the LAS in measuring aerosol number concentration. An aqueous KCl solution was atomized and dried to create the polydisperse aerosol. Sample flow was extracted from the chamber simultaneously by the LAS and a TSI 3010 condensation particle counter (CPC). Number concentration reported by the LAS was compared to reported values from the CPC to determine accuracy in measurement of total particle number concentration.

2.5.3. Sample Train Flow

To verify that all sampling was performed isokinetically, dilution was accurate, and wait time during upstream/downstream switching was accurate, flow rates in the sample train were measured. Flow was measured with a DC-1 Piston Meter (Bios International Co., Butler, NJ).

A critical orifice was located immediately upstream of the vacuum pump to regulate the total flow rate in the sample train. To ensure accurate operation of the orifice, airflow was passed through a HEPA filter prior to entering the orifice. The orifice was designed to provide three lpm of flow. Flow was measured upstream of dilution, upstream of each valve at the wye, and downstream of the wye after sample extraction by the LAS (Figure 2.4).

Figure 2.4: Sampling points for calibration of sample train



2.6. Bio-TEC Characterization

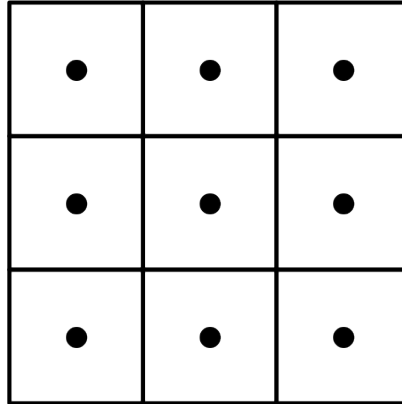
2.6.1. Background Aerosol Concentration

To verify that the pre-filtration of section of the Bio-TEC provided a contaminant-free gas stream for testing, ambient total number concentration in the chamber was measured prior to aerosol generation. The Bio-TEC was operated for 30 minutes to equilibrate the system and remove any residual contaminants in the chamber. Following the equilibration period, total number concentration was measured with the CPC inside the chamber.

2.6.2. Uniformity of Face Velocity and Aerosol Concentration

Uniformity of face velocity and aerosol concentration in the Bio-TEC was characterized prior to testing any air purification devices. As defined in ASHRAE Method 52.2, a nine-section traverse was defined for the cross-sectional face of the chamber. Measurements were recorded from the center of each equally sized section (Figure 2.5).

Figure 2.5: Nine-section traverse for measuring face velocity and aerosol concentration



In accordance with the ASHRAE standard, the coefficient of variation for both face velocity and aerosol concentration was verified to be less than 10%.

$$CV = \frac{Std. Dev.}{Mean} \quad \text{Eq. 6}$$

where:

CV = Coefficient of Variation

Std. Dev. = Standard deviation of the nine-section traverse

Mean = Mean of the nine-section traverse

2.7. Particulate Removal Efficiency

In order to account for potential losses due to impaction or settling within the air purification devices, removal efficiency was calculated using downstream measurements as described below. With the air purification device installed in the Bio-TEC, the aerosol generation device was started and gas flow was established at the desired rate in the Bio-TEC. With the purification device “off,” aerosol concentration was monitored at the downstream sample location. Once a uniform aerosol concentration was established, measurements were recorded without operating the purification device. This measurement was used to establish downstream concentration without active operation of the air purification device. Next, the air purification device was activated, and measurements were recorded with active purification.

Because this work is concerned with the removal of bioaerosols from building air streams, diameter dependent particulate removal efficiency was calculated. A size range of 0.5 to 1.5 μm diameter was selected using the LAS. Particle removal efficiency was determined using Eq. 7.

$$PRE = \left(1 - \frac{C_{on}}{C_{off}} \right) \times 100 \quad \text{Eq. 7}$$

where:

PRE = particle diameter dependent (graded) removal efficiency

C_{on} = downstream number concentration of particulate matter with specified diameter with device on

C_{off} = downstream number concentration of particulate matter with specified diameter with device off

2.7.1. *AEI Particle Removal Efficiency*

The AEI device was evaluated for aerosol particle removal efficiency in the Bio-TEC. During testing, airflow was held constant at 25 CFM (0.71 m^3/min), actual conditions. The device was controlled by an audio amplifier with 24 user-selectable gain settings. Power to the acoustic system was controlled by adjusted the gain-dial on the amplifier. Amplifier gain settings were then correlated to measured power consumption by the in line power meter.

Removal efficiency was first determined during operation at full power and then at subsequent reduced power settings. Data was collected at the maximum and minimum gain settings and at six equally spaced intervals between the maximum and minimum. During operation, sound pressure level in the ambient environment was monitored 1 m from the center of the Bio-TEC system. Sound pressure level was measured with a handheld digital sound level meter (Model SM-100, Dwyer Instruments, Michigan City, IN) capable of measuring 30 to 130 dB with an accuracy of ± 1.5 dB.

2.8. Calculation of Annualized Operational Cost

A comparison of energy cost for HEPA filtration, AEI, and EEI technologies is beneficial. Costs were calculated for a hypothetical application in a building requiring 5,000 CFM (141.6 m³/min) airflow. Estimated cost of HEPA filtration was calculated by determining required break horsepower to overcome the static pressure of the HEPA filter (Eq. 8).²⁷ This method was also used to calculate cost due to pressure drop and power requirements for sound generation for the AEI device.

$$BHP = \frac{Q_F \times SP}{6356 \times FAN_{EFF}}$$

where:

Eq. 8

BHP = Break Horsepower

Q_F = flow rate into the filter (CFM)

SP = static pressure of HEPA filter (in W.G.)

FAN_{EFF} = Fan efficiency (assumed to be 75% in this calculation)

Calculated break horsepower was utilized in the determination of total yearly operational costs. For this calculation an assumed electrical rate of \$0.15 /kWh was used (Eq. 9).

$$\frac{Cost}{Year} = BHP \left(\frac{0.746 kW}{1 BHP} \right) \left(\frac{24 h}{1 day} \right) \left(\frac{365 days}{1 year} \right) \left(\frac{\$0.15}{1 kWh} \right)$$

Eq. 9

Real annualized cost for operation of the AEI device was determined by summing cost due to pressure drop and calculated energy cost as determined by measured, at-the-wall power consumption. These results were compared with estimates based on projected energy costs for operation as provided by the equipment manufacturer.

3. RESULTS AND DISCUSSION

3.1. Interpretation of ASHRAE Method 52.2

After close inspection of the ASHRAE 52.2 standard, several key parameters were selected for use in the design of the reduced-scale test chamber. Based on the equipment to be tested, it was determined that the Bio-TEC should be constructed with a front cross-section-area of 7” x 7” (17.8 cm x 17.8 cm). These included total residence time as it relates to particle settling velocity, Reynolds numbers associated with specific chamber segments, and airflow face velocity in the chamber.

3.1.1. Terminal Settling Velocity of KCl

The terminal settling velocity for KCl particles was calculated for spherical diameters of 0.5 to 1.5 μm (Eq. 10). Calculations were performed based on normal laboratory conditions (air at temperature 293K, pressure 101.2 kPa). Density of KCl particles is taken as 1.98 g/cm^3 . Stokes regime was assumed for all particles. This assumption was validated by calculating Reynolds number for particles based on theoretical terminal settling velocity (Figure 3.1).

$$v_t = \frac{m_p C_C g}{3 \pi \mu d_p} \quad \text{Eq. 10}$$

where:

v_t = terminal settling velocity (cm/s)

m_p = particle mass (g)

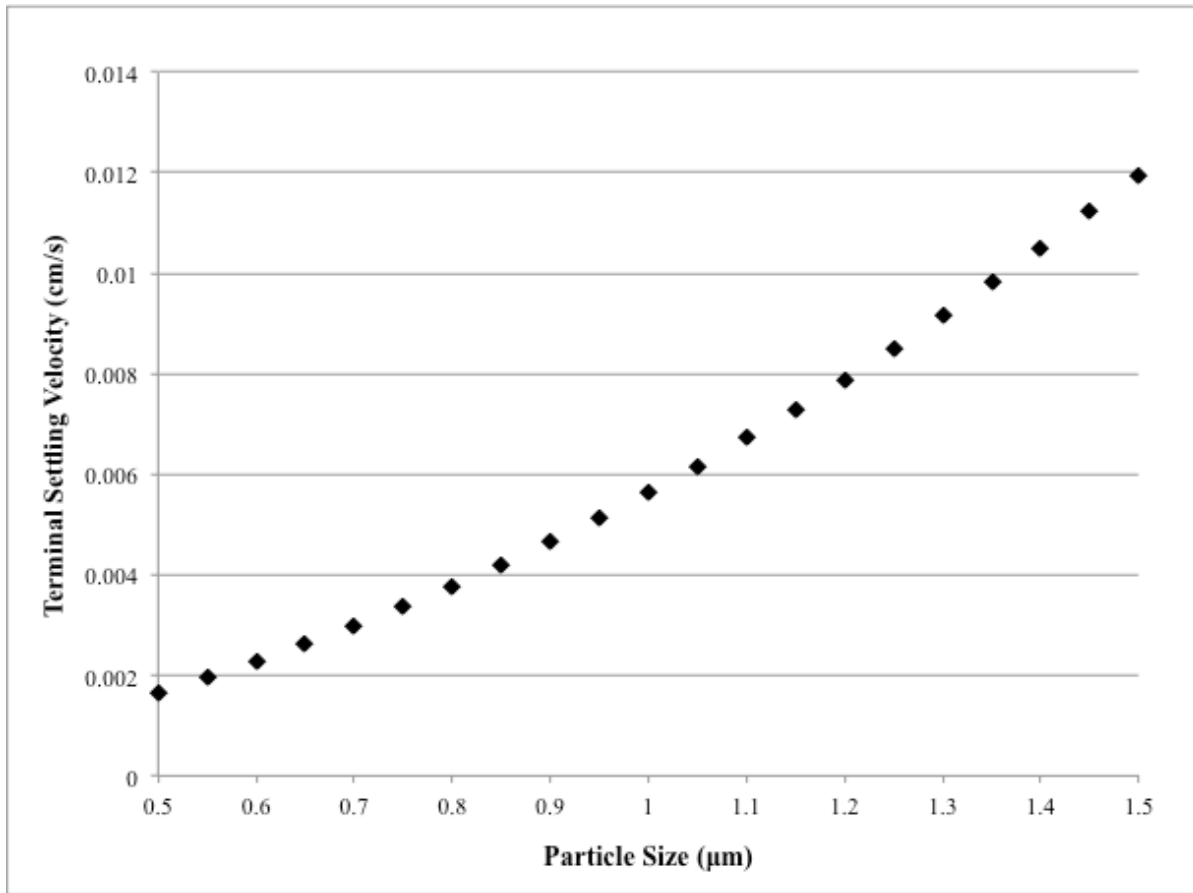
C_C = Cunningham Correction Factor

g = acceleration due to gravity (cm/s^2)

μ = viscosity of fluid ($\text{g}/\text{cm}\cdot\text{s}$)

d_p = diameter of particle (cm)

Figure 3.1: Theoretical terminal settling velocity as calculated with Eq. 10



Calculated velocities were used to ensure that particles would not prematurely settle from the air stream and collect at the bottom of the chamber. The calculation was performed assuming that flow was laminar. Particles will more readily settle due to gravity under laminar flow conditions, so this represents a “worst case scenario” in the chamber. When modeling gravitational settling in turbulent flow conditions, a duct is assumed to be “well-mixed” in the vertical and horizontal directions and contain only a small laminar-flow boundary edge. When particles are transferred from the well-mixed region to the laminar region they are considered to be removed from the system. Settling in both laminar and turbulent flow conditions are dependent on the fractional efficiency of the chamber (Eq. 11).³⁸

$$FE = \frac{v_t CSA_C}{Q_C}$$

where:

Eq. 11

FE = fractional efficiency

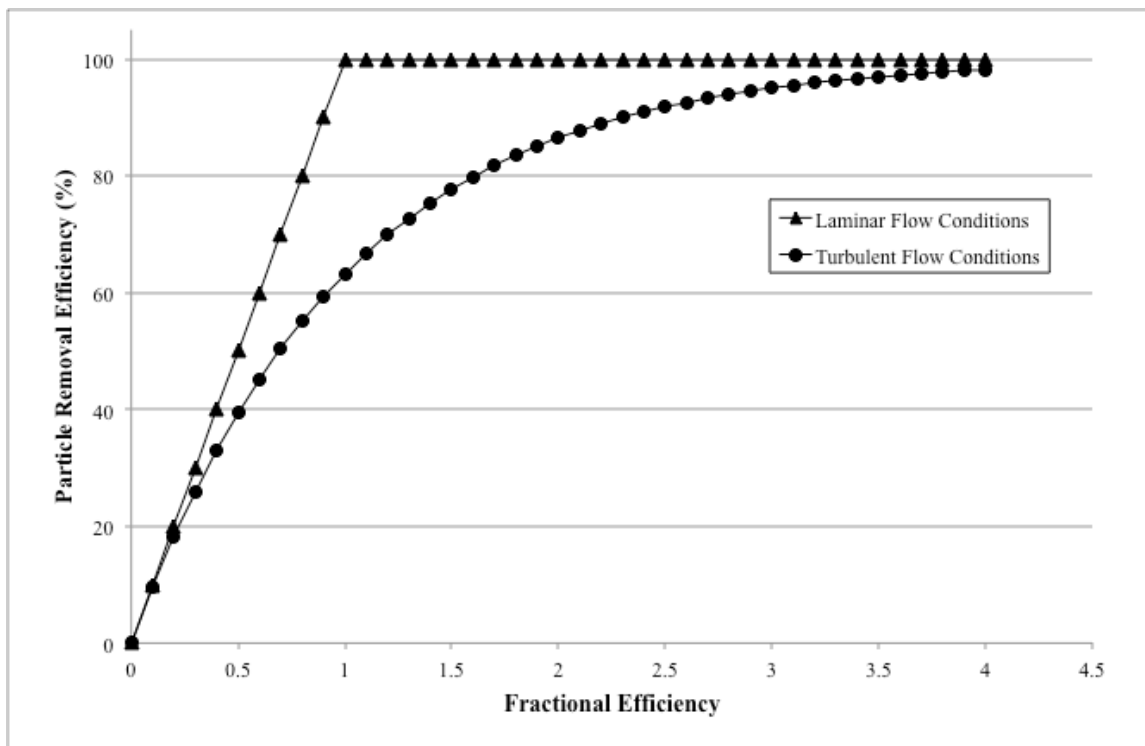
v_t = terminal settling velocity (m/s)

CSA_C = cross sectional area of the chamber (m²)

Q_C = actual flow inside chamber (m³/s)

Graded collection efficiency of a laminar-flow chamber is linearly dependent on the fractional efficiency of the chamber. For turbulent-flow chambers, removal efficiency is exponentially dependent on fractional efficiency. Because of the exponential dependence in turbulent flow conditions, particle removal efficiency in a turbulent flow chamber will asymptotically approach the removal efficiency of a laminar flow chamber with the same fractional efficiency (Figure 3.2).

Figure 3.2: Comparison of particle removal efficiency under laminar and turbulent flow conditions



Because all sections of the Bio-TEC are designed to exhibit full turbulent flow, it is expected that particle settling due to gravity will be minimal. For example, the particle removal efficiency for worst case conditions of $d_p = 1.5 \mu\text{m}$ ($v_{tp} = 0.012 \text{ cm/s}$), $A = 1,050 \text{ cm}^2$ (collection area upstream of device), and $Q = 11,800 \text{ cm}^3/\text{s}$ (flow rates used in this paper) results in collection efficiency in the test chamber without the particle removal devices of 6.3% and 6.1% for laminar and turbulent flow conditions, respectively.

3.1.2. Total Gas Residence Time

The residence time of an air parcel in the ASHRAE standard was used as a guide for the scaled Bio-TEC design. Based on guidelines in the standard, chamber sections where length was restricted were be the aerosol inlet, upstream mixing, downstream mixing, and sample port sections as defined in Figure 3.3. Sections designed for pre and post filtration and flow generation were not restricted by the ASHRAE standard. In the Bio-TEC, these unrestricted sections were only required to have a residence time sufficiently low so as to make particle loss due to settling negligible. If residence time is too long, test aerosols settle from the air stream, causing inflated removal efficiency calculations. The residence times were calculated based on the low end of the targeted flow rates for each system. For the ASHRAE method, the low flow is 472 CFM ($13.4 \text{ m}^3/\text{min}$) at actual conditions. For the Bio-TEC the low flow is 10 CFM ($0.471 \text{ m}^3/\text{min}$) at actual conditions. Unless otherwise specified, all flow rates presented are at actual conditions.

Table 3.1: Residence times calculated at lowest flow for ASHRAE Method and Bio-TEC. Section locations correspond to the diagram presented in Figure 3.3

Section	System	Residence Time (s)	Length (in)	Length (cm)
Aerosol Inlet	ASHRAE	1.02	24	61.0
	Bio-TEC	1.19	7	17.8
Upstream Mixing	ASHRAE	3.57	84	213.4
	Bio-TEC	3.91	23	58.4
Downstream Mixing	ASHRAE	3.57	84	213.4
	Bio-TEC	3.91	23	58.4
Sampling	ASHRAE	0.51	12	30.5
	Bio-TEC	0.68	4	10.2

3.1.3. *Reynolds Number*

The Reynolds number of the ASHRAE standard was determined for both high and low flow rates. At both test airflow rates, the main mixing section of the chamber is fully turbulent, with $Re \gg 4,000$ (7.4×10^5 to 3.7×10^6). The ASHRAE Duct utilizes fully turbulent flow to mix the test aerosol. This is important to ensure that mixing is uniform and adequate for testing. Therefore, all segments of the Bio-TEC were designed with Reynolds number exceeding 4,000. The range of calculated values of Reynolds number for the Bio-TEC system was 6.1×10^4 to 3.1×10^5 at 10 and 50 CFM (0.471 and 2.36 m³/min) actual, respectively. The calculated Reynolds number for indicates fully turbulent flow over the operational range of the Bio-TEC.

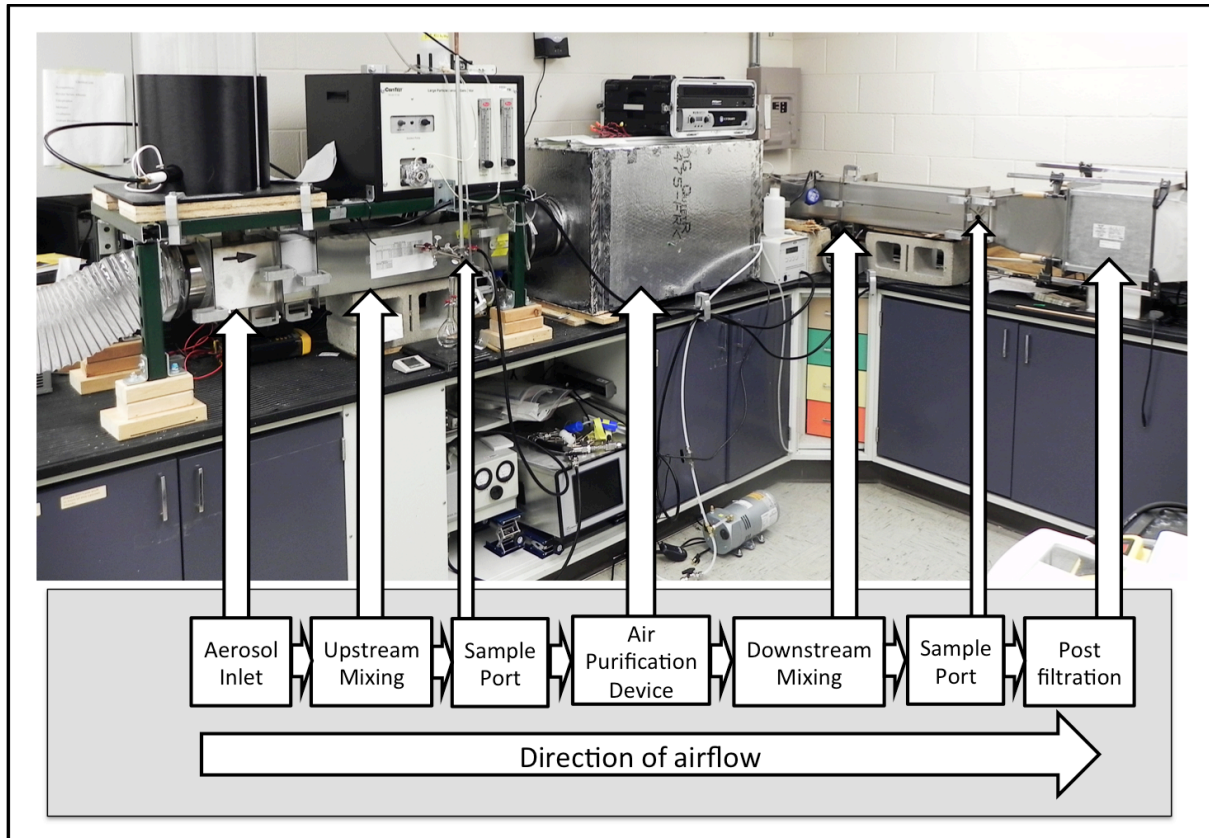
3.2. Design and Assembly of Bio-TEC

3.2.1. *Bio-TEC Segment Design*

Based on calculations to determine Reynolds number, face velocity, and residence time, individual segments of the Bio-TEC were designed. The main sections of were fabricated with a square cross-sectional profile of 7" x 7" (0.18 x 0.18 m). Each section was terminated with a 1" (2.54 cm) flange. A complete library of Bio-TEC segment designs is provided in Appendix A.

The Bio-TEC was assembled on the surface of a lab bench. To prevent potential conductivity between the chamber and the bench surface, a thick rubber mat was used to completely cover the bench surface. Because of the varying size of air purification devices to be tested, it was necessary to vary the distance of the Bio-TEC centerline above the bench. Lab jack stands were used to level the chamber.

Figure 3.3: Photograph of complete Bio-TEC with main components highlighted. The flow generation and pre-filtration sections are located out of the image on the left side



Adjoining sections of the Bio-TEC were connected using four clamps, one positioned at each corner (Figure 3.3). All connecting sections were treated with foam gaskets prior to connection. After the clamps were tightened, all seals were leak tested by over-pressurizing the Bio-TEC by 3.2 cm H₂O and visually inspecting with Snoop Liquid Leak Detector (Swagelok Co., Solon, OH) with no bubbles detected visually.

Figure 3.4: Three sections of the Bio-TEC coupled with clamps. The flanges are gasketed with a closed cell foam material



The EEI and AEI systems have inlet and outlet openings that are not the same dimensions as the test chamber. Therefore, it was necessary to construct transition sections to allow for swapping systems for testing without disrupting the flow regime and aerosol mixing. All transition sections were designed to contract or expand at no greater than a 7° angle to prevent aerosol impaction or uneven concentration distribution.

3.2.2. Material Properties

All sections of the Bio-TEC were fabricated from type 304 brushed stainless steel. To prevent particle charging or electrostatic deposition of particles onto the walls of the Bio-TEC, it is important that all materials that contact the testing air stream are fabricated from conductive material and effectively grounded. Sample probes and pressure taps were also fabricated from stainless steel materials. Stainless steel was chosen both because of its conductive

properties as well as its resistance to corrosion. Because the test aerosol is crystalline KCl, corrosion is a potential issue with any equipment.

After assembly, an electrical continuity check was performed across the entire system. In places where there was a lack of electrical continuity, electrical connections were completed by soldering a conductive bridge between adjoining non-continuous sections. The completed chamber was connected to earth ground via an adjacent electrical raceway. Using the Scopemeter, all adjacent chamber sections were verified to have electrical continuity. Depending on its material characteristics, when an air purification device is installed for testing electrical continuity may be disrupted. Therefore, the Bio-TEC was connected to earth ground both upstream and downstream of the device location.

3.2.3. *Flow Generation*

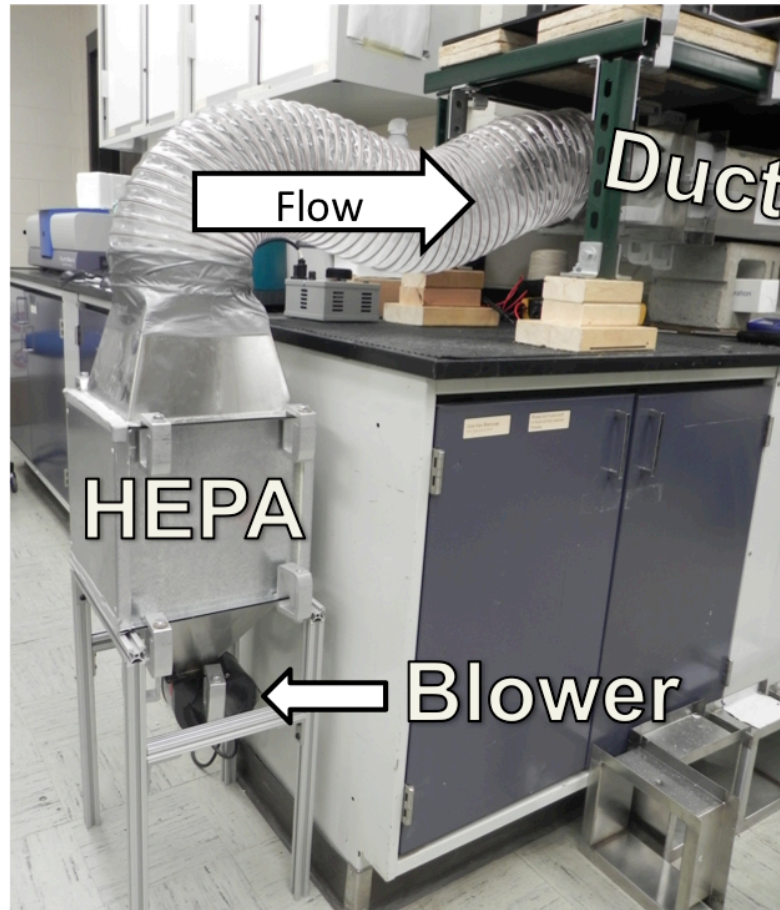
In contrast to the ASHRAE standard, the Bio-TEC was designed as an open system utilizing HEPA-filtered room. As such, all tests were performed at room temperature, humidity, and total pressure. These conditions are 21 to 23 °C, 40 to 60 % relative humidity, 100.2 to 102.3 kPa. The effluent air stream was also HEPA-filtered at the post-filtration stage to remove any remaining test aerosols prior to release into the room.

The airflow was generated with a forced draft, powered by a 146 CFM (4.1 m³/min) direct drive PSC blower (Model 1TDP7, Grainger Industrial Supply, Lake Forest, IL) operated at 115V and 60Hz. Blower speed was controlled with a variable voltage controller (120V Statco 3PN501B, Statco Co., Dayton OH) to set test airflow rates. Due to space constraints, the blower was mounted in a vertical position (Figure 3.5).

As previously mentioned, Outlet flow from the blower was passed through a HEPA filter to remove particulate contamination. After HEPA filtration, the flow was directed to the centerline of the Bio-TEC using conductive flexible plastic tubing. The tubing was transitioned to the Bio-TEC with a round to rectangular segment and attached with a hose clamp. While connecting the flexible tube to the stainless steel transition segment, small tears in the plastic were observed. To prevent leakage at this point, duct sealer (Scotch Duct Sealer

900 3M, St. Paul, MN) was applied to the inside of the tube prior to attachment. Any tears were subsequently covered with the sealer, and the connection was tested for leaks with Snoop and visual inspection.

Figure 3.5: Vertical orientation of the blower and HEPA pre-filtration stage prior to Bio-TEC connection via conductive tubing

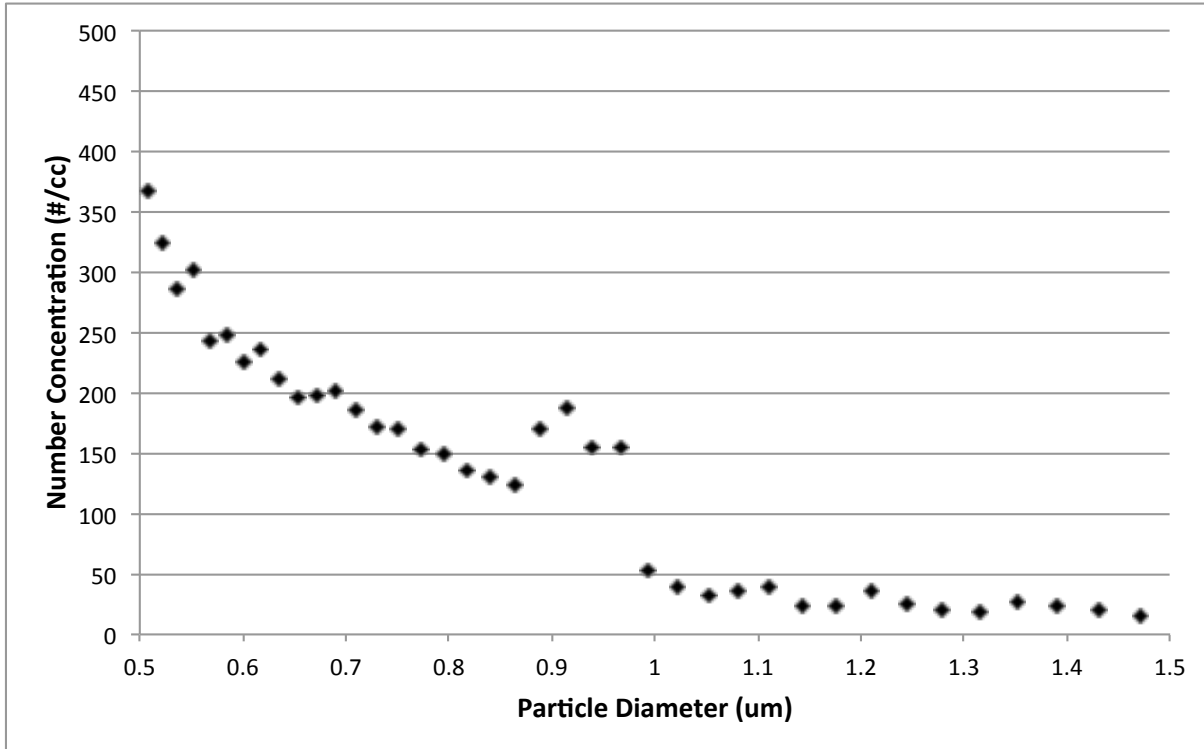


3.3. Aerosol Generation

A 30% KCl by weight solution was prepared with deionized water and aerosolized with the Large-Particle Aerosol Generator. During aerosol challenges, the aerosol generator was operated with the peristaltic pump at setting “1”, atomizing air at 1 CFM (0.028 m³/min), and drying air at 5.83 CFM (0.165 m³/min). The surrogate aerosol was required to contain polydisperse sized particles. Because the goal of this work is to determine removal efficiency of aerosols that are most challenging to remove based on size and includes many bioaerosols,

the size range of interest is 0.5 – 1.5 μm in diameter. Aerosol polydispersion was validated with the LAS prior to testing (Figure 3.6).

Figure 3.6: Data confirming the presence of a polydisperse aerosol from 0.5 - 1.5 μm in diameter



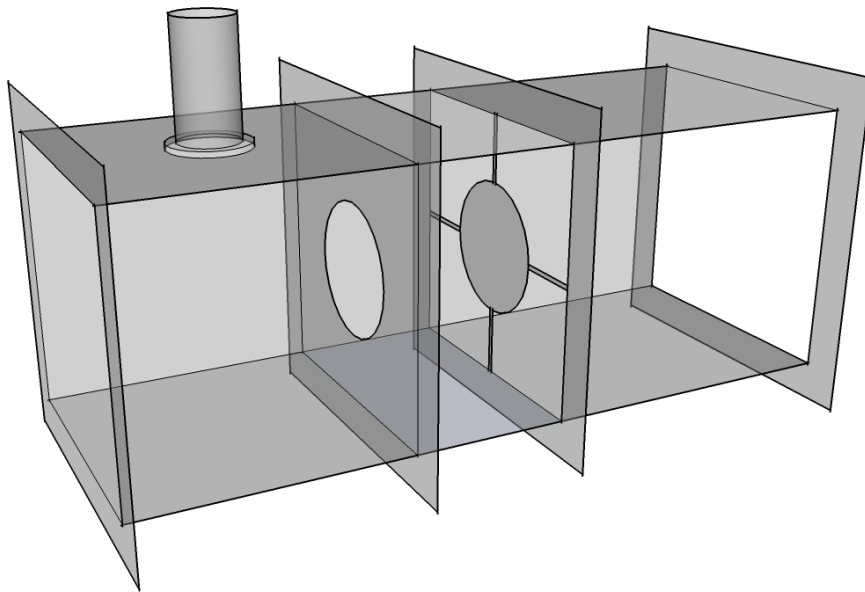
The challenge aerosol was introduced to the Bio-TEC immediately downstream of initial HEPA filtration. The drying column was directly connected to the top of the chamber with a stainless steel nipple.

As a safety precaution, a CPC was used to monitor total number concentration at the outlet of the downstream HEPA filter. The CPC was operated to continuously sample room air 0.5 m away from the center of the Bio-TEC's outlet. If a leak were to occur at any connection, it is important to stop system operation quickly to reduce cross-contamination with other experiments in the lab.

After initially checking the uniformity of the aerosol concentration at the upstream sampling port, it was determined that both aerosol concentration and face velocity maintained a maximum at the center of the chamber. During initial characterization of airflow uniformity, a coefficient of variation of 23.8% was measured. Flow velocity around the internal perimeter of the chamber, 1.2" (3.0 cm) from the edge, was, in some areas, reduced to less than 60% of the centerline velocity.

To reduce the edge effect and help establish a uniform velocity and concentration profile in the chamber, an orifice plate was located 6" (15.2 cm) downstream of aerosol injection (Figure 3.7). The orifice was circular and centered in the Bio-TEC.³⁷ The plate covered 50% of the cross-sectional chamber area. A perforated stainless steel diffusion plate was attached to the downstream side of the mixing orifice to further assist mixing. All surfaces of the mixing orifice and diffusion plate were coated with vacuum grease to prevent re-aerosolization of impacted particles. After installation of the orifice and diffusion plates, the coefficient of variation at 10 CFM (0.283 m³/min) was calculated to be 6.9% and was considered acceptable for future tests.

Figure 3.7: Aerosol inlet and mixing – computer aided design (CAD) drawing of chamber sections at the aerosol inlet. Test aerosol enters through the nipple at the top left. Flow is from left to right



The aerosol generation equipment can also be modified to create polydisperse particles of different concentrations and compounds, or monodisperse aerosols from PSL spheres. This may be useful for future work in the Bio-TEC that requires different, or potentially more specific analysis.

3.4. Aerosol Sampling Equipment

3.4.1. Isokinetic Sampling Ports

Samples were drawn from the Bio-TEC with the vacuum pump. Sample flow was maintained at 3 lpm by a critical orifice located immediately upstream of the pump. Because the chamber was designed to be operated at varying flow rates, it was necessary to fabricate sample ports of different sizes to ensure isokinetic sampling at all flow rates.

Table 3.2: Sizes of sample ports for varying Bio-TEC flow rates

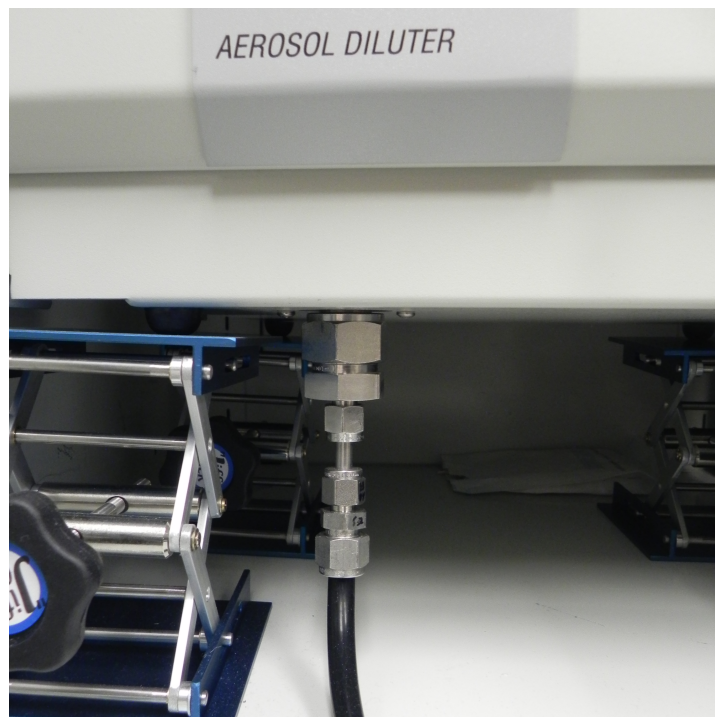
Bio-TEC Flow (CFM)	Bio-TEC Flow (m ³ /min)	Sample Probe Area (in ²)	Sample Probe ID (in)	Sample Probe Area (cm ²)	Sample Probe ID (cm)
50	1.42	0.10	0.36	0.67	0.92
40	1.13	0.13	0.41	0.84	1.03
30	0.85	0.17	0.47	1.12	1.19
20	0.57	0.26	0.57	1.67	1.46
10	0.28	0.52	0.81	3.35	2.06

When testing at 50, 40, or 30 CFM (1.42, 1.13, or 0.85 m³/min), the same sample probe was used. The probe was one cm in inner diameter. This was possible because the required size at each flow rate were near the same size. The use of an inexact probe will cause sub- and super-isokinetic sampling depending on the chamber flow rate, but the particle size ranges affected by this sampling artifact would lie outside of the diameter size range of interest. For particles with 1 μm diameter, this will cause no more than 18% over sampling or under sampling, depending on the flow rate.³⁹ However, since all data are collected at constant flow rates any increase or decrease in sample will be realized while sampling with the device on and off.

3.4.2. Dilution and Analysis with LAS

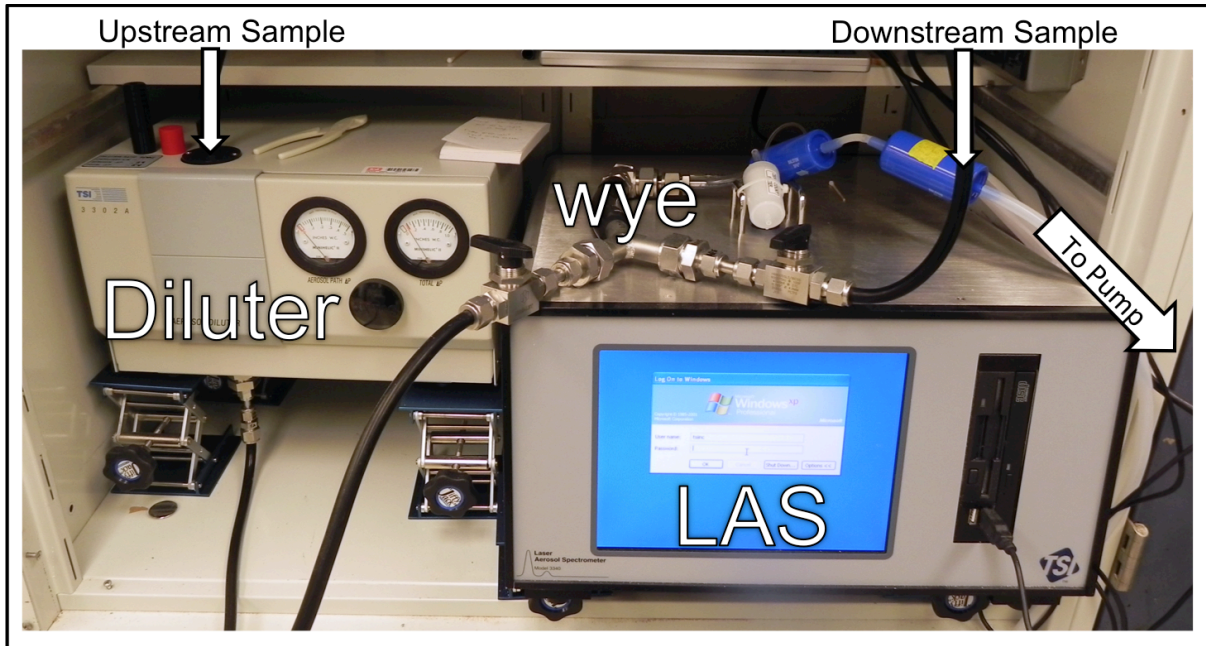
After sample extraction with the stainless steel isokinetic ports, samples were transported in conductive rubber tubing. Upstream samples were passed through a dilution step prior to analysis. Downstream samples were routed directly to the LAS for analysis. The diluter was designed for direct attachment to a TSI APS. However, the setup used for aerosol sampling in the Bio-TEC did not require use of an APS. Because no APS was used, the diluter did not come with standard connections that were adequate to operate it in the sample train without an APS. Therefore, a special fitting was made to allow the equipment to be used for in-line dilution without an APS. (Figure 3.8)

Figure 3.8: Outlet of aerosol diluter modified for in-line use



After dilution, upstream or downstream samples were selected at the manually controlled wye. The wye was placed immediately upstream of the LAS so when a switch was performed between sampling locations the residual would be removed from the sample line within 18 sec.

Figure 3.9: Image of diluter, wye, laser aerosol spectrometer (LAS), and pump flow direction for sampling equipment

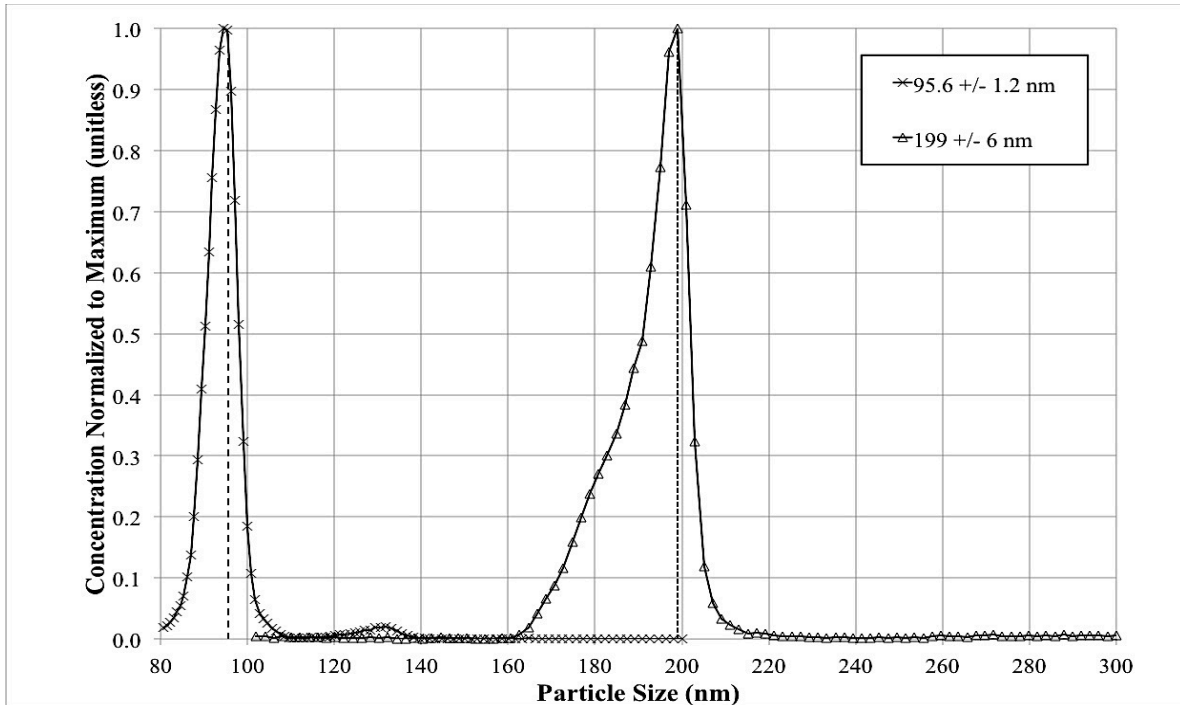


3.5. Equipment Calibration and Validation

3.5.1. LAS Sizing Accuracy

Optical particle sizing equipment is often limited in ability to accurately determine sub-micrometer particle diameters. Because of this concern, the LAS was calibrated in the lab to determine its ability to accurately measure the diameter of sub- μm particles. Two sizes of PSL spheres were used for this test. Sizes used were $95.6 \pm 1.2 \text{ nm}$ and $199 \pm 6 \text{ nm}$ in diameter. Experiments for each size were carried out separately, and the data was aggregated into one plot and compared with the standard (Figure 3.10).

Figure 3.10: LAS Calibration – measured particle diameter from the LAS compared with NIST-traceable PSL particle standards



Based on data collected during this experiment it was determined that the LAS was capable of accurately sizing particles of 0.956 μm and 0.199 μm diameter within 4%. This result was better than anticipated, and indicates that measurements collected with the LAS during air purification device testing in the Bio-TEC can be expected to have excellent accuracy with respect to particle diameter.

3.5.2. LAS Number Concentration Accuracy

Accuracy of LAS number concentration was validated by aerosolizing PSL spheres and operating the LAS in parallel with a CPC. To ensure that the instrument was accurate across the entire size range of interest, this calibration procedure was again performed with 95.6 +/- 1.2 nm and 199 +/- 6 nm NIST traceable PSL spheres, as well as a polydisperse aerosol from a 30% by weight KCl solution. Average number concentration over 1 min as measured by the LAS remained within $7.6 \pm 4\%$ of the CPC values.

3.5.3. Flow Rates in Sample Train

As previously mentioned, flow rates at key points in the aerosol sample train were carefully measured with a piston meter. At each sample location the piston meter was connected and tested for leaks prior to measuring. The vacuum pump and LAS were both turned in. The pump was expected to draw 3 lpm as controlled by the critical orifice. The LAS was expected to draw 0.1 lpm, controlled by an internal critical orifice. The piston meter was set to perform 10 sequential measurements and the average was recorded (Table 3.3).

Table 3.3: Measured flow rates at key points in sample train at actual conditions

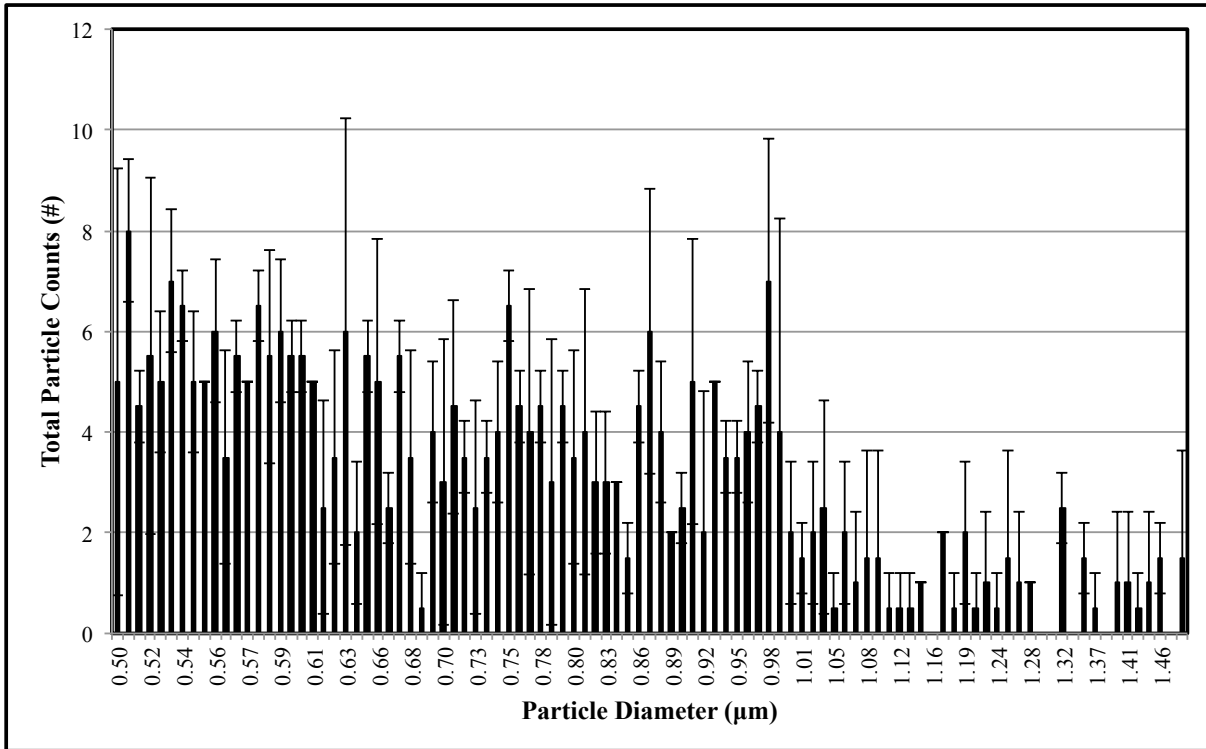
Location	Location Description	Flow Rate (lpm)
1	Upstream of diluter	2.917
2	Upstream line to wye	2.948
3	Downstream line to wye	2.926
4	Immediately upstream of wye	2.885

All measurements taken upstream of the LAS were within 0.083 lpm of the expected value. This is a difference of no more than 2.8%, depending on the location. The deviation of the final measurement, immediately upstream of the pump, was slightly farther from 3 lpm, but only deviated by 3.8% from the expected value. Because the LAS withdrew 0.1 lpm, it was expected that measurement location 4 would exhibit an average flow rate 0.1 lpm lower than those measured upstream of the LAS.

3.5.4. Bio-TEC Background Concentration

Prior to generation of aerosols, care was taken to ensure that chamber leakage would not affect accuracy of particle removal efficiency measurements. Flow was established at 25 CFM (0.71 m³/min), and the chamber was allowed to equilibrate for 30 minutes prior to measurement with the LAS. Samples were extracted at the upstream port but were not diluted prior to analysis. Each trial was performed for 5 min. Measurements were performed in triplicate and mean values were plotted with standard deviation (Figure 3.11).

Figure 3.11: Prevalence of background aerosol in the Bio-TEC presented as total particle counts in each size bin during a 5 min sample while withdrawing sample at 3,000 cm³/min and sampling at 180 cm³/min



When compared to the average aerosol concentration profile presented in Figure 3.6, the background levels are negligible and will not significantly affect the accuracy of measurements. At all size ranges of interest the background concentration is at least four orders of magnitude lower than the concentration of the test aerosol.

3.6. Characterization of AEI Device

When operating at full power, the device consumed 850 W. Subsequent measurements were taken at reduced power levels. Ambient sound pressure was measured at 1m during device operation. The maximum level never exceeded 68dB. Static pressure drop due to the AEI system was 0.47” H₂O (1.2 cm H₂O) measured during operation at 25 CFM (0.71 m³/min).

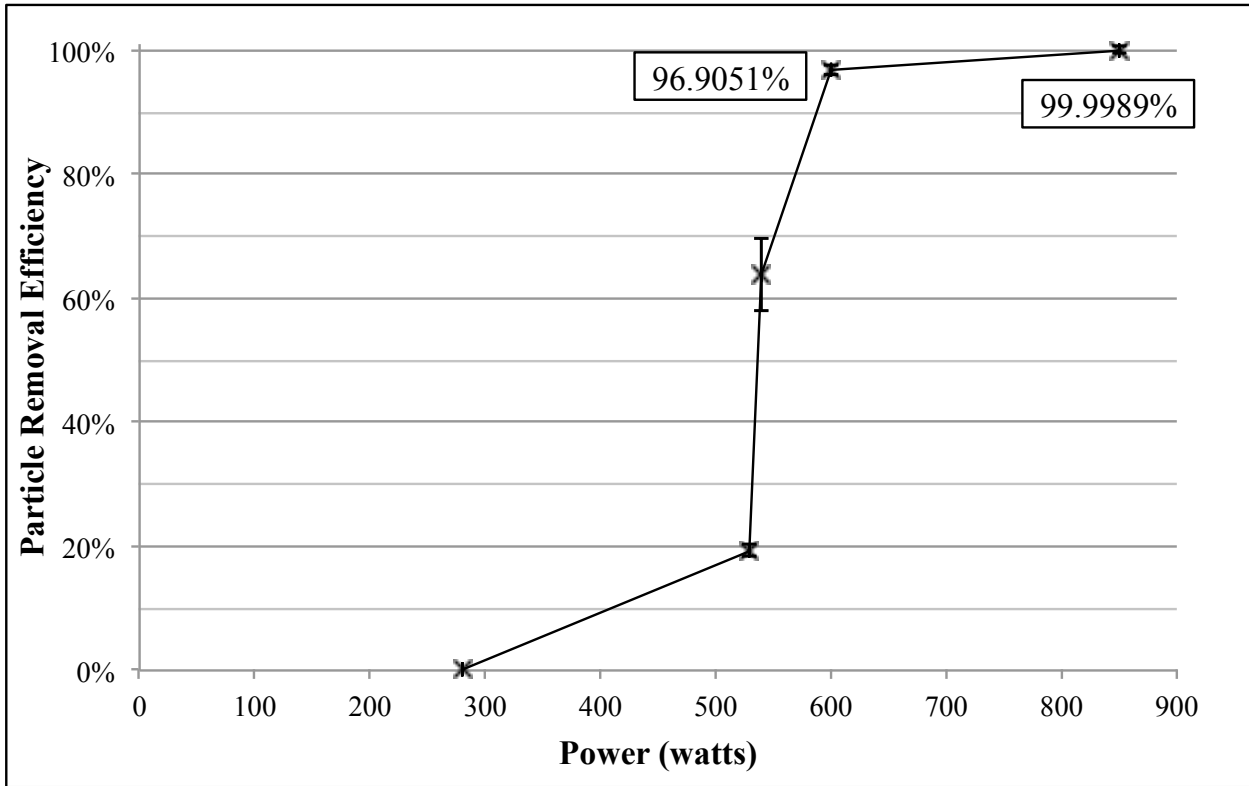
Particle removal efficiency by the AEI device without a sound field was determined prior to testing with the sound field applied. Measurements were performed in triplicate, and the mean particle removal efficiency of the device was calculated. When operated at 25 CFM

(0.71 m³/min) without the sound sources powered, the AEI device removed 71.2% ± 8.3% of particles in the 0.5 to 1.5 µm diameter range based on number concentration. This removal efficiency corresponds to that of an average in-home fabric filter.³⁷

When it was not powered, the AEI system was capable of removing particles by the tortuous gas flow path through the sound-dampening section of the device as well as by collection on the coarse filter media. Inspection of the first sound-dampening panel on the upstream side of the device provided visual evidence of particle collection on the foam-like material. Collection on the sound-dampening panel may cause premature corrosion of the material depending on chemical composition of collected particles.

Aerosol particle removal efficiency was measured relative to at-the-wall operating power. Testing was completed at an airflow rate of 25 CFM (0.71 m³/min). At full power, the AEI device was capable of 99.9989% removal of particles from 0.5 to 1.5 µm diameter. Operation at 70% of total power yielded 96.905% particle removal of the same size range. All measurements were performed in triplicate. Mean removal efficiency and standard deviation were calculated for the 0.5 to 1.5 µm diameter particle size range (Figure 3.12).

Figure 3.12: AEI removal efficiency vs. power for 0.5-1.5 μm diameter particles. Standard deviations, noted by vertical lines are too small to see for all test conditions except 540 W. Particle removal efficiency values achieved when the device is not powered on are not included in this figure



Removal efficiency data collected with the AEI air purification device demonstrate a promising capability of particulate removal with a modest pressure drop across the device. When operated at full power, the device was capable of exceeding removal efficiency standards prescribed for HEPA filtration equipment that require 99.997% particle removal for particles with diameter larger than 0.3 μm .

While not presented in Figure 19, it was observed during operation of the device that removal efficiency of particles larger than 1.5 μm in diameter was nearly 100%. Initially, a set of experiments was performed to determine the particle size range should of interest. During this experiment, data was collected to determine removal efficiency for particles from 0.5 to 10 μm in diameter. Of the three trials, total particle counts above 1.5 μm never exceeded 8 for a 5 min sample time. This is in comparison to an average of 2,950 counts for the size bins

covering 0.5 to 1.5 μm diameter particles for the same sample duration. The high collection efficiency for large particles indicates that an effective design may include upstream filtration with a rough filter to remove large particles prior to purification by the AEI device. This would likely extend operational lifetime of the AEI device and reduce clogging caused by aggregation of large particles inside the device.

Because of the simple “drop in” design and minimal required modifications to HVAC equipment during installation, the AEI device could be used as an alternative where HEPA is already in place. A simple sound-dampening baffle installed at the inlet and outlet of the device reduced sound pressure level to a point where it is not detectable over other mechanical equipment noises.

Interestingly, the particle removal efficiency caused only by the sound pressure is maintained above 80% when the device is operating with only about 65% of total power consumption. In a normal office environment, 80 to 90% of room air is recirculated without filtration, while only 10 to 20% is comprised of filtered fresh air.⁴⁰ Purification of recirculated air may be as important as purification of fresh air intake in designing a building for protection from external attack by BWAs. For instance, if a biological contaminant is present externally to the building envelope, it can be carried inside by building leakage or airflow wakes traveling behind occupants during ingress, after which the HVAC system can rapidly disperse the contaminant throughout the building.

3.7. Cost Analysis

Determination of an estimated annualized cost for operating HEPA filters is difficult. The main cost in operating HEPA filtration equipment is incurred due to the power required for the HVAC fan to overcome the static pressure of the filter. Filter static pressure may vary greatly with specific filter used due to variations in pleating, fabric depth, and overall surface area exposed to the airflow.⁴¹ Generally speaking, as the exposed surface area of the filter is reduced, the pressure drop caused by the filter is increased.³⁹ Due to physical size constraints for air filtration equipment, filter design for specific applications can vary greatly. Therefore,

cost calculations for operation of HEPA filters can only be accurately calculated on a case-by-case basis.

Design of a facility with a high level of protection from BWAs with currently available technologies may increase total facility construction cost by 30%.⁴² This includes a complete system utilizing HEPA filtration, a zoned HVAC system, air locks, active HVAC controls, and particulate sensing equipment. Assuming an average capital cost of \$150 per square foot for a standard office facility, a 5,000 ft² (464.5 m²) building would have an added first cost of \$225,000 for a complete Collective Protection system. A system such as this is designed to operate HEPA filtration equipment for supply air only when triggered by sensing equipment.

A power budget for the first generation AEI system was calculated based on measured values of at-the-wall energy consumption of 800 W and pressure drop across the system of 0.47” H₂O (1.2 cm H₂O). Data were used to calculate anticipated annualized cost (\$/yr) for full time operation of the AEI device. For comparison, the estimated annualized budget was compared with that of a typical HEPA filtration system (Table 3.4). Pressure drop across an unused, new HEPA filter is no more than 1” H₂O (2.54 cm H₂O)⁴¹. A used HEPA filter that has been in service and collected a significant filter cake can have a pressure drop of 4” H₂O (10.16 cm H₂O) or higher.⁴¹ For the purposes of this calculation a used HEPA filter is characterized by static pressure of 4” H₂O (10.16 cm H₂O).

Table 3.4: Annualized cost of AEI device compared with clean and dirty HEPA filtration

Device	Energy (kW)	Annualized Energy (kWh/yr)	Annualized Cost (\$/yr)
AEI Total	1.168	10,228	1,534
Pressure	0.368	3,220	483
Sound	0.800	7,008	1,051
New HEPA	0.782	6,852	1,028
Used HEPA	3.129	27,406	4,111

The AEI device currently exists in a first-generation. Applied Research Associates, the developer of the AEI system, has started to design improvements in the piezoelectric sound source manufacturing process to increase the efficiency of the system. It is anticipated that the redesigned sound source, coupled with modified flow through designs to reduce static pressure of the device may lead to a reduction in operational costs equal to an order of magnitude or greater. Sound sources designed to output a more narrow-band frequency and the inclusion of a custom designed Helmholtz resonator will increase efficiency for conversion of the electrical signal to sound pressure. Additionally, more finely tuned sound sources will allow for a higher sound pressure level to be attained at an equal power input. With higher sound pressure levels, the flow through channels can be enlarged to reduce overall pressure drop of the system.

A projected cost estimate for the AEI and EEI devices has been prepared. Energy used by the systems was obtained from modeled projections provided by the vendors. After the design and fabrication of the second-generation AEI device is completed it is anticipated the device will require 0.06 J/L to generate the sound for treatment of a contaminated air stream. Increased efficiency in sound generation will allow for larger flow-through cavities, thus reducing the total pressure drop caused by the system. Pressure drop has the potential to be reduced to 50% of the first-generation system (personal communication with Mr. Jason Gallia, ARA Inc.). The EEI device is anticipated to require approximately 0.13 J/L to treat an air stream and will induce a negligible pressure drop (personal communication with Ms. Pooran Tepper, Sentor Inc.). In comparison, new HEPA filters require 1 J/L. Annualized cost was again calculated to compare operational expenses for the different technologies (Table 3.5).

Table 3.5: Estimated annualized operational costs for second generation AEI air purification technology and EEI device based on vendors anticipated energy requirements. Costs are estimated based on electricity price of \$0.15 per kWh

Device	Annualized Energy (kWh/yr)	Annualized Cost (\$/yr)
New HEPA	6900	1,035
Used HEPA	27400	4,110
AEI	2810	422
Pressure	1610	242
Sound	1200	180
EEI	2700	405

Utilization of an energy efficient approach for collective protection such as AEI or EEI air purification devices may yield an alternative approach that allows for continuous protection without relying on sensor systems. Because sensor-triggered active control of HVAC zones is not required with this approach, the total first-cost of a system would be comprised of only the capital cost of the purification device. Based on current estimates provided by the manufacturer, it is estimated that for both the AEI and EEI technologies a 5,000 CFM (141.6 m³/min) system would cost less than \$100,000. This represents a capital savings of approximately \$125,000 when compared to a traditional protection approach.

Traditional protection techniques frequently overlook bioaerosol transport due to ingress and instead focus strategies on purification of incoming fresh air with HEPA filtration and UV sterilization. By utilizing an AEI device in the recirculation ducting and maintaining, or potentially increasing, air change rates, it may be possible to significantly reduce transport of bioaerosols within a building. If the device is operated at 65% power, the additional energy load to the building is expected to be minimal compared to typical building energy demands, but indoor/outdoor aerosol concentration ratios may be significantly reduced.

In situ particle agglomeration by acoustic radiation is well documented in the literature.^{30,31,43} Although not investigated in this study, it is hypothesized that air purification by AEI induces aerosol agglomeration. Agglomerates < 0.5 μm in diameter may not be collected in the

system and be transported within the indoor environment. Before agglomeration, these particles would not be captured by EEI, but if the air stream passes first through an acoustic device and then into the EEI equipment it may be possible to increase removal efficiency of these particles.

Removal efficiency data for EEI are not presented in this paper because the evaluation has not yet been completed. However, the technology is presented for consideration because of similar potential applications with the AEI. It is also possible that the use of AEI and EEI in series may lead to previously unrealized purification capabilities.

4. SUMMARY AND CONCLUSIONS

4.1. Summary of Research Results

A testing and evaluation chamber was designed to provide a modular system for testing air purification devices at low airflow rates for potential use in biological protection applications. In conforming to many of the constraints established in the ASHRAE 52.2 method for particle removal efficiency testing, the Bioaerosol Testing and Evaluation Chamber (Bio-TEC) represents an excellent tool for low cost evaluations of prototype devices. The flexible modularity of the system allows for equipment of varying size, pressure drop, and required airflow rates to be evaluated. The aerosol generation equipment can also be modified to create polydisperse test particles of different concentrations and compounds, or monodisperse test aerosols from polystyrene latex (PSL) spheres. Careful calibration and validation procedures were performed to minimize the effects of aerosol deposition due to settling, electrostatic charge, chamber leakage, and excess background contaminant levels. Steps taken during fabrication and validation to ensure a uniform velocity and concentration profile throughout the complete cross sectional area of the chamber.

Additionally, removal efficiency and energy requirements of an Acoustically Enhanced Impaction (AEI) air purification device was evaluated in the new Bio-TEC. The device was capable of removing 99.9989% of 0.5 to 1.5 μm diameter KCl particles representative of the particle size range of interest for particles that are difficult to remove from gas streams based on size and for bioaerosol removal. This exceeded the performance requirement of 99.997% particle removal efficiency as defined for high efficiency particle air filters. Pressure drop of the AEI device was measured to be 0.47" H_2O (1.2 cm H_2O) measured during operation at 25 CFM (0.71 m^3/min). A cost analysis was prepared to compare operational expenses of AEI with that of HEPA filtration. The total annualized operational cost due to pressure drop and sound generation for AEI is \$1,534 as compared to \$1,028 for a new HEPA filter and \$4,111 for a used HEPA filter with an established filter cake.

The AEI device has the potential to serve as an important component in a complete Collective Protection (ColPro) system. AEI has the potential to be used in either continuous operation (100% duty cycle) or sensor triggered air purification device. While capital costs of an AEI

system would likely exceed the first cost of standalone high efficiency particulate air (HEPA) filtration equipment, a traditional ColPro system utilizing HEPA filters requires a zoned heating ventilation and air conditioning (HVAC) system and a sensor network to trigger filter activation. The additional systems are utilized in traditional systems to limit energy costs for filtration and reduce maintenance requirements for filter changes. With a projected power budget of at least an order of magnitude lower than HEPA filters, an AEI device could be operated continuously without the need for sensors and active zone control in an HVAC system.

4.2. Future Work

While power consumption of the AEI device was measured in this study, we anticipate significant reductions in power needed to achieve the same particle collection efficiency with the implementation of a new sound source. Work is currently underway to develop a modified piezoelectric transducer capable of similar sound pressure output with a reduced power requirement. Preliminary projections have estimated that that the new sound source, coupled with other minor design modifications, has the capability to reduce power consumption by an order of magnitude or greater. With these modifications, the AEI device is projected to operate with an energy requirement that is at least 60% less than HEPA filtration.

Device reliability under extended operation at a 100% duty cycle will be evaluated at the bench-scale prior to pilot-scale testing. It is anticipated that, with inclusion of the new sound source, the AEI device will be capable of operating maintenance free for longer intervals than HEPA filters. An AEI system could be implemented similar to a filter baghouse with multiple independent devices operating in parallel. By cycling sound on and off in the devices the filters can be self-cleaned.

A concept system would utilize five AEI devices operating simultaneously. The chamber containing contaminated airflow would pass through a manifold to direct independently to each of the five devices. Dampers downstream of the devices can be used to control whether the treated air is directed back into the building airflow or exhausted from the system. While

four devices would be operating to remove particles from the airstream, one device would pass the airstream without sound treatment. When the sound is off, captured particles are released. This air stream could be exhausted to the external environment or subsequently treated with a disinfection system such as dry thermal heating or germicidal ultraviolet (UV) exposure. A system operated in this setup has the potential to reduce maintenance costs for replacement filters and man hours needed to check and maintain operation of the filtration equipment.

A complete study of the Electrospray Enhanced Impaction (EEI) device will be completed with the Bio-TEC system once the equipment is received to complete the testing. The transition section for the EEI device, that is needed to test the device, has been designed and is described in Appendix A.

Based on results from this work, an integrated pilot-scale system will be designed in cooperation with the Department of Defense Joint Program Manager for Collective Protection (JPM-ColPro). JPM Col-Pro operates a test facility in a controlled environment that replicates a normal office-building environment with fully functioning HVAC equipment.

A hybrid Computational Fluid Dynamics (CFD) and zonal modeling effort is being completed synchronously with bench-scale device evaluations to simulate contaminant transport through the pilot-scale facility. Based on experimental results from the bench-scale system, the model will be run with varying inputs to determine optimum placement of air-purification devices, recirculation rates, and device power in a typical office building. This will be used as a tool during the scale-up process to develop a complete concept of operation. It will be used to make recommendations for implementation based on the modeled capability to control indoor transport of biological warfare agents in an economically effective way.

5. REFERENCES

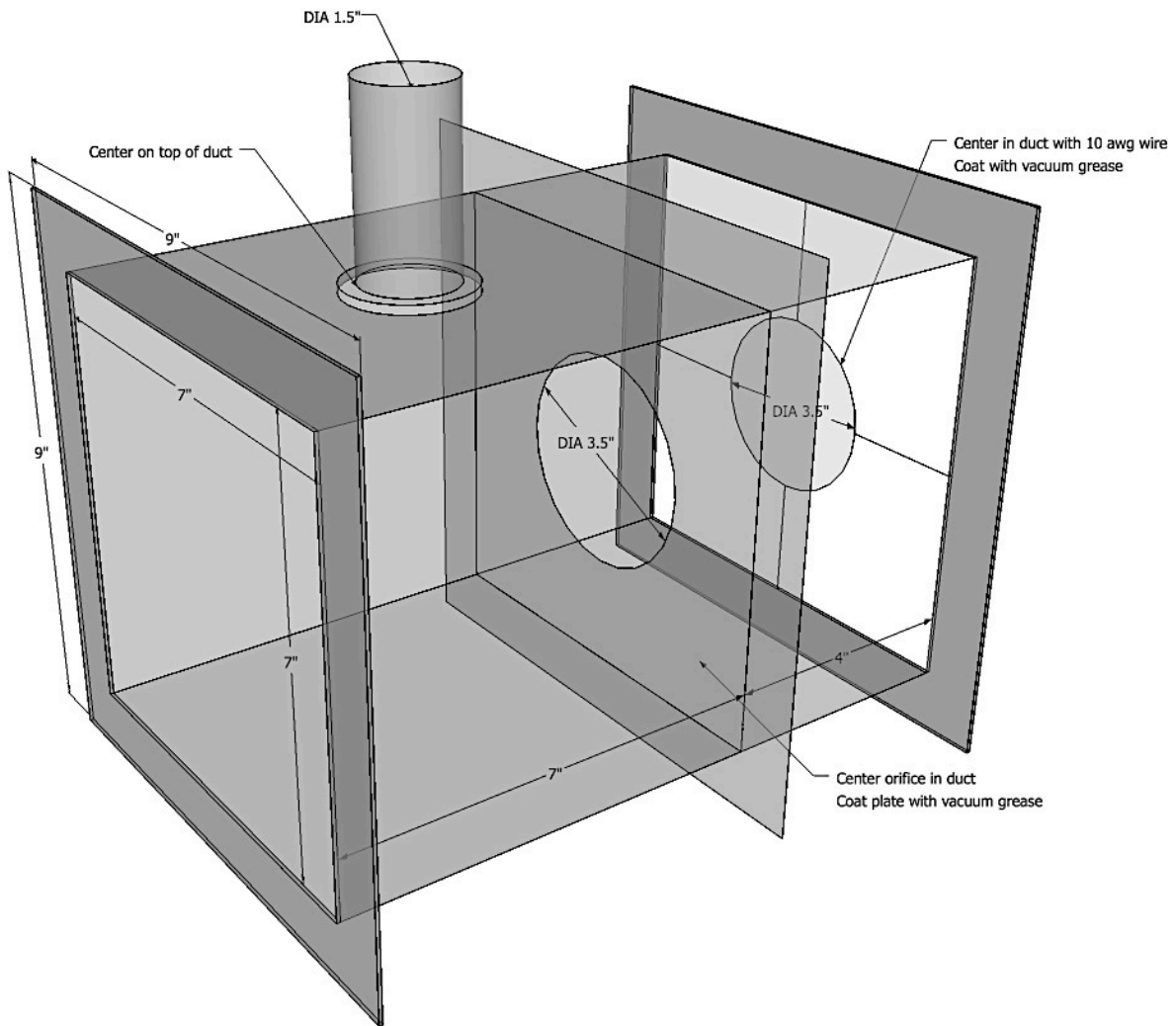
- 1 *Homeland Security Presidential Directive 10*; The White House, Office of the Press Secretary, 2004.
- 2 Demirev, P.A.; Feldman, A.B.; Lin, J.S. *J. Hopkins Apl. Tech. D.* **2005**, *26*, 321-333.
- 3 Takahasi, H.; Keim, P.; Kaufmann, A.F.; Keys, C.; Smith, K.L.; Taniguchi, K.; Inouye, S.; Kurata, T. *Emerg. Infect. Dis.* [online] **2004**, *10*.
<http://www.cdc.gov/ncidod/eid/vol10no1/03-0238.htm> (accessed Feb 22 2011).
- 4 Fitch, J.P.; Raber, E.; Imbro, D.R.; *Science* **2003**, *302*, 1852-1853.
- 5 Mayor, S.D.; Benda, P.; Murata, C.E.; Danzig, R.J. *Biosecur. Bioterror* **2008**, *6* 25-46.
- 6 Bryden, W. *Immune Building Program* NDIA Collective Protection Conference, Monterrey, CA, June 21, 2005. http://proceedings.ndia.org/5460/5460/1_bryden.pdf (accessed March 3, 2011).
- 7 Warner, T.; Benda, P.; Swerdlin, S.; Knieval, J.; Argenta, E.; Aronian, B.; Balsley, B.; Bowers, J.; Carter, R.; Clark, P.; Clawson, K.; Copeland, J.; Crook, A.; Frehlich, R.; Jensen, M.; Liu, Y.; Mayor, S.; Meillier, Y.; Morley, B.; Sharman, R.; Spuler, S.; Storwold, D.; Sun, J.; Weil, J.; Xu, M.; Yates, A.; Zhang, Y. *Bulletin of the American Meteorological Society* **2007**, *88*, 167-176.
- 8 Centers for Disease Control and Prevention: Bioterrorism agents/diseases, <http://www.bt.cdc.gov/agent/agentlist-category.asp> (accessed Feb 20, 2011).
- 9 Yee, E.; Kosteniuk, P.R.; Roy, G.; Evans, B.T.N. *Appl. Optics* **1992**, *31*, 2900-2913.
- 10 Gittins, C.M.; Piper, L.G.; Rawlins, W.T.; Marinelli, W.J.; Jensen, J.O.; Akinyemi, A.N. *Field Anal. Chem. Tech.* **1999**, *3*, 274-282.
- 11 Tepper, G.; Kessick, R.; Pestov, D. *J. Appl. Phys.* **2007**, *102*, 113305-1.
- 12 Cooper, C.D.; Alley, F.C. *Air Pollution Control: A Design Approach*, 3rd ed.; Waveland: Long Grove, IL, 2002.
- 13 Fisk, W.J.; Faulkner, D.; Palonen, J.; Seppanen, O. *Indoor Air* **2002**, *12*, 223-234.
- 14 Tinsley, B.A.; Zhou, L.; Plemmons, A. *Atmospheric Research* **2006**, *79*, 266-295.
- 15 Noh, K.; Park, J.; Jung, Y.; Yi, S.; Huang, J. *Aerosol and Air Quality Research* **2011**, *11*, 80-89.

- 16 Tepper, G.; Kessick, R. *J. Aerosol Sci.* **2008**, *39*, 609-617.
- 17 Chang, J.; *J. Electrostatics*, **2003**, *57*, 273-291.
- 18 Zuraimi, M.S.; Tham, K.W. *Build. Environ.* **2009**, *44*, 2475-2485.
- 19 Weschler, C.J. *Indoor Air* **2000**, *10*, 269-288.
- 20 Boelter, K.J.; Davidson, J.H.; *Aerosol Science and Technology* **1997**, *27*, 689-708.
- 21 Maximum Acceptable Level of Ozone. *Code of Federal Regulations*, Part 801, Title 21, Volume 8, 2010.
- 22 Weschler, C.J.; Shields, H.C.; Shah, B.M. *J. Air Waste Ma.* **1996**, *46*, 291-299.
- 23 *Guidance for Protecting Building Environments from Airborne Chemical, Biological, and Radiological Attacks*; Pub No. 2002-139; National Institute for Occupational Safety and Health: Cincinnati, OH, 2002.
- 24 Evans, B.T.N., Yee, E., Roy, G., and Ho, J.: Remote detection and mapping of bioaerosols, *J. Aerosol Sci.*, *25*(8), 1549-1566, 1994.
- 25 Sohn, M.D.; Sextro, R.G.; Gadgil, A.J.; Daisey, J.M.; *Indoor Air* **2003**, *13*, 267-276.
- 26 Airaksinen, M.; Kurnitski, J.; Pasanen, P.; Seppanen, O. *Indoor Air* **2004**, *14*, 92-104.
- 27 Bell, A.A. Jr.; *HVAC: Equations, Data, and Rules of Thumb*, 2nd ed.; McGraw Hill: New York, NY, 2008.
- 28 Meegan, G.D.; Gallia, J.R. *Acoustic Fractionator-Based Air Purification*, Proceedings of the Chemical and Biological Defense Physical Science and Technology Conference, New Orleans, LA, Nov 17-21, 2008.
- 29 Goddard, G.; Kaduchak, G. *J. Acoust. Soc. Am.* **2005**, *117*, 3440-3447.
- 30 Holwill, I.L.J. *Ultrasonics*, **2000**, *38*, 650-653.
- 31 Whitworth, G.; Coakley, W.T. *J. Acoust. Soc. Am.* **1992**, *91*, 79-85.
- 32 Gallia, J.; Meegan, D.; Zadler, B. *Acoustic Fractionator Air Purification System*; Final Report to ERDC-CERL on Contract W9132T-10-C-0012; Applied Research Associates: Littleton, CO, 2010.

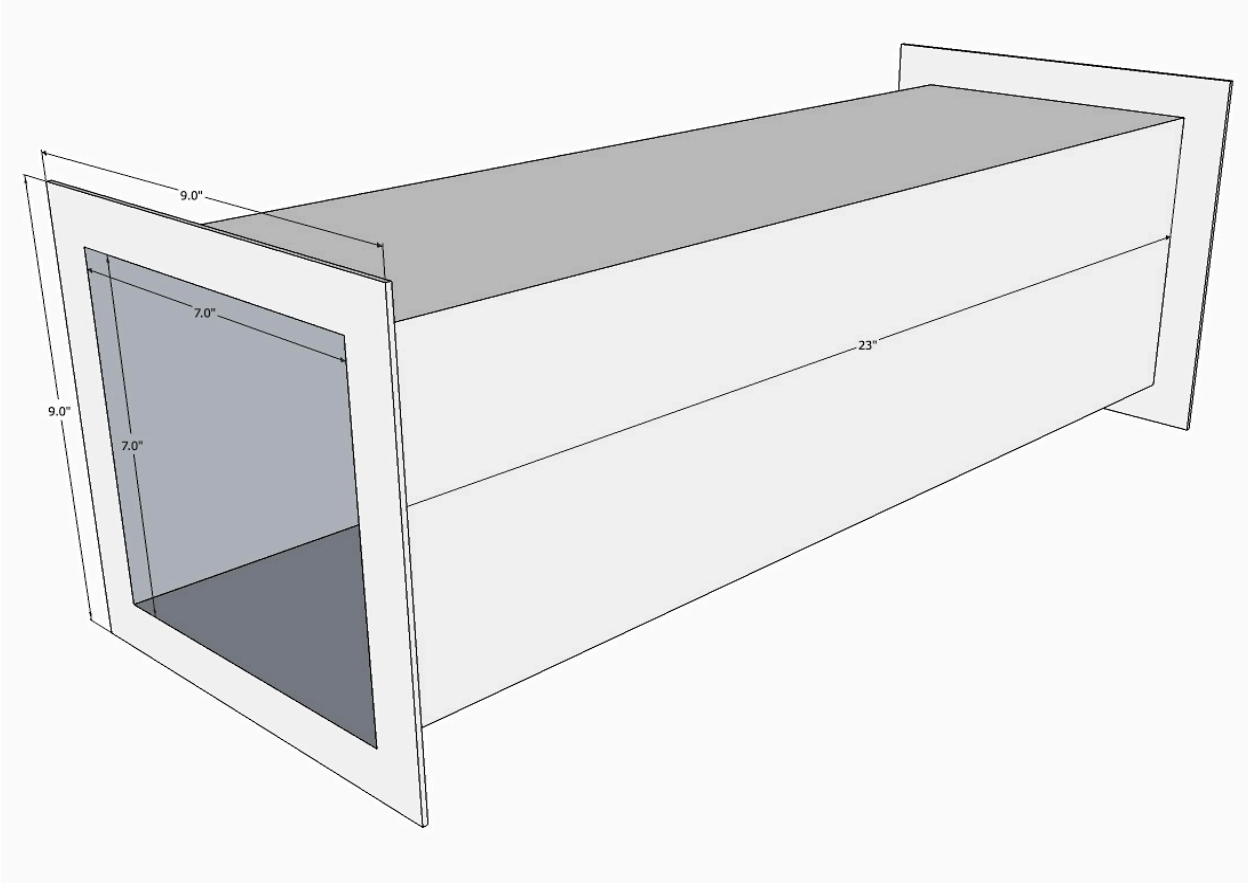
- 33 Fenn, J.B.; Mann, M.; Meng, C.K.; Wong, S.F.; Whitehouse, C.M. *Science* **1989**, *246*, 64-71.
- 34 Smith, R.D.; Barinaga, C.J.; Udseth, H.R. *Anal. Chem.* **1988**, *60*, 1948-1952.
- 35 Tepper, G.; Fenn, J.; Kessick, R.; Pestov, D.; Anderson, J.; *IEEE-Nano* **2006**, *2*, 781-782.
- 36 Kim, J.H.; Lee, H.S.; Kim, H.H.; Ogata, A.; *J. Electrostatics* **2010**, *68*, 305-310.
- 37 *ANSI/ASHRAE Standard 52.2-2007: Method of Testing General Ventilation Air-Cleaning Devices for Removal Efficiency by Particle Size*; American Society of Heating, Refrigerating and Air-Condition Engineers, Inc.; Atlanta, GA, 2007.
- 38 Wark, K.; Warner, C.F.; Davis, W.T. *Air Pollution Its Origin and Control*, 3rd ed.; Longman: New York, 1998; pp 220-225.
- 39 Zhang, Y.; *Indoor Air Quality*; CRC Press: Boca Raton, FL., 2005.
- 40 Zuraimi, M.S.; Weschler, C.J.; Tham, K.W.; Fadeyi, M.O.; *Atmos. Environ.* **2007**, *41*, 5213-5223.
- 41 Rudnick, S.; *Aersol Sci. Technol.* **2004**, *38*, 861-869.
- 42 *Unified Facilities Criteria: Security Engineering: Procedures for Designing Airborne Chemical, Biological, and Radiological Protection for Buildings*; UFC 4-024-01; US Army Corps of Engineers, 10 June, 2008.
- 43 Liu, J; Zhang, G.; Zhou, J; Wang, J.; Zhao, W.; Cen, K.; *Powder Technol.* **2009**, *193*, 20-25.

APPENDIX A: SCHEMATICS OF BIO-TEC SECTIONS

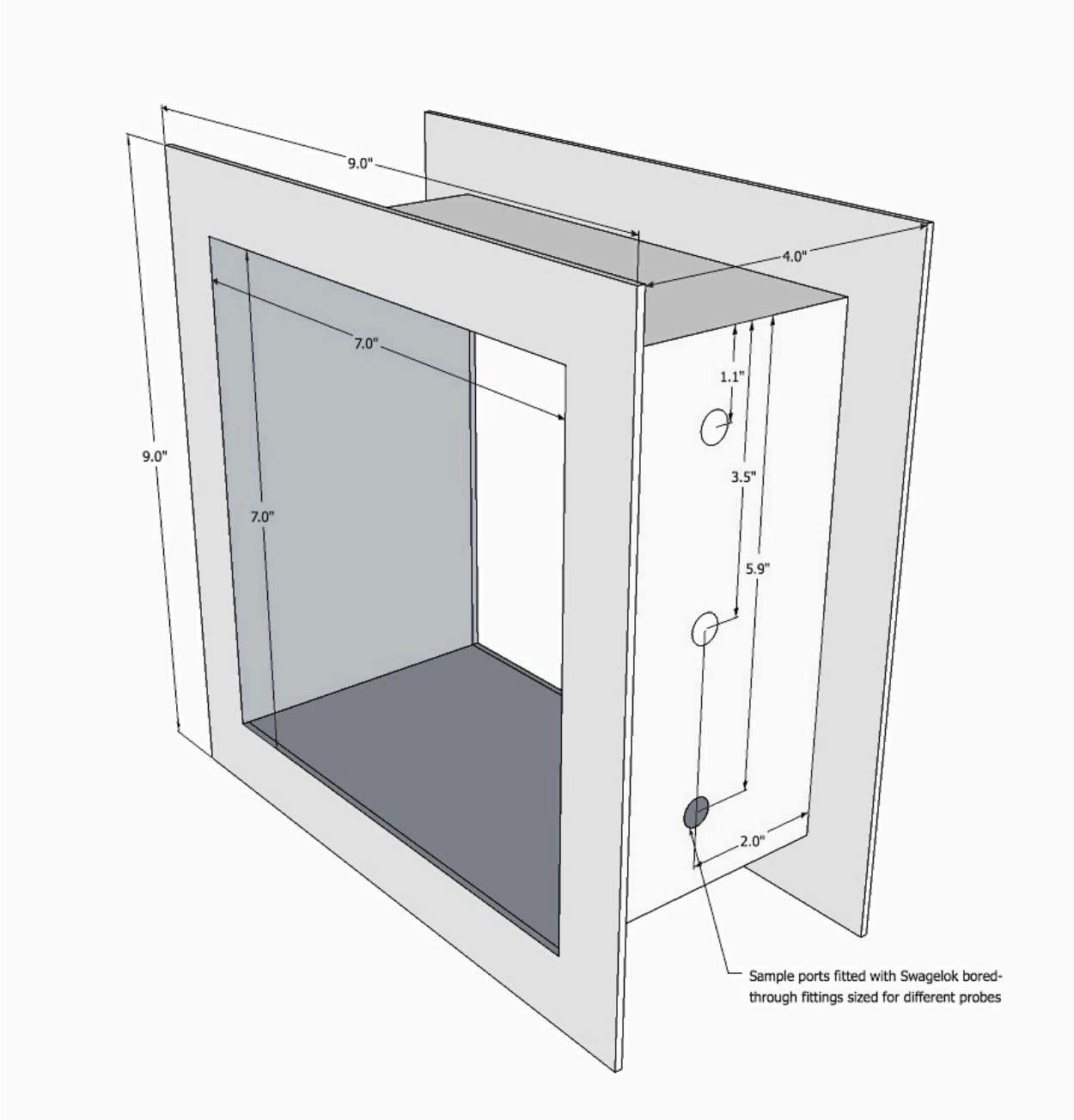
Aerosol inlet section



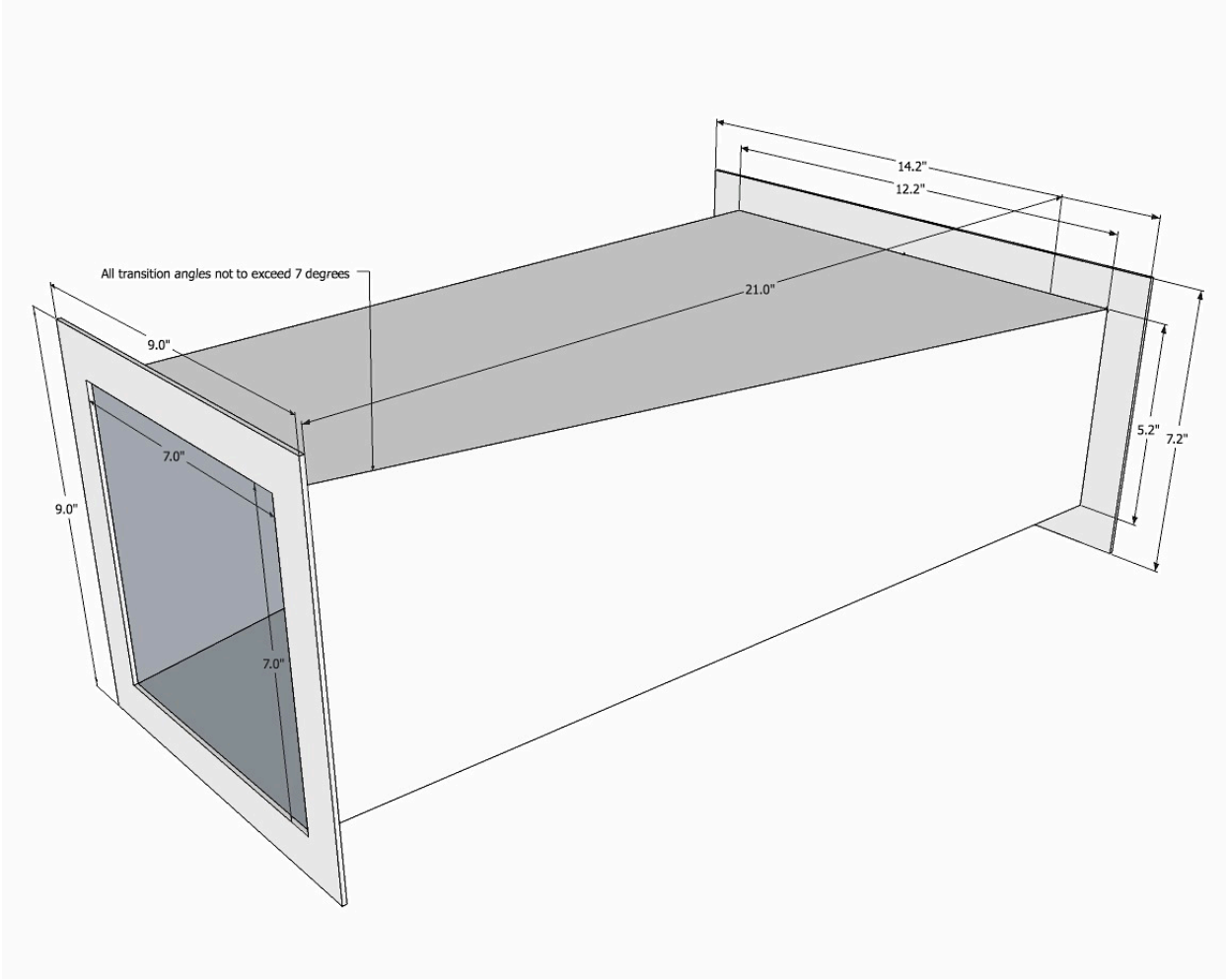
Upstream and downstream turbulent mixing sections



Sampling section



Reducing transition section



Downstream 90° turn section

